American Journal of Chemical Engineering
2021; 9(3): 53-78
http://www.sciencepublishinggroup.com/j/ajche
doi: 10.11648/j.ajche.20210903.12
ISSN: 2330-8605 (Print); ISSN: 2330-8613 (Online)

CO_2 Valorization Reactions over Cu-Based Catalysts: Characterization and the Nature of Active Sites

Ubong Jerome Etim[1], Raphael Semiat[1, 2, *], Ziyi Zhong[1, *]

[1]Guangdong Technion Israel Institute of Technology (GTIIT), Shantou, China

[2]Wolfson Faculty of Chemical Engineering, Technion – Israel Institute of Technology, Haifa, Israel

Email address:

ziyi.zhong@gtiit.edu.cn (Ziyi Zhong), cesemiat@technion.ac.il (R. Semiat)

[*]Corresponding author

To cite this article:

Ubong Jerome Etim, Raphael Semiat, Ziyi Zhong. CO_2 Valorization Reactions over Cu-Based Catalysts: Characterization and the Nature of Active Sites. *American Journal of Chemical Engineering*. Vol. 9, No. 3, 2021, pp. 53-78. doi: 10.11648/j.ajche.20210903.12

Received: May 25, 2021; **Accepted**: June 7, 2021; **Published**: June 21, 2021

Abstract: Active sites are the individual reactors at the molecular scale distributed on the heterogeneous catalyst surface. To a large extent, they determine the catalytic performances and the reaction pathway of a reaction. Therefore, understanding the nature and structure of the actives sites is crucial to improve and develop novel, robust and practical catalysts. The wide application of state-of-the-art characterization techniques these years makes it possible to obtain crucial information about the active sites for some catalysts. The Cu-based catalysts are widely used for water gas shift (WGS) and methanol synthesis from syngas ($CO + H_2$). Although having some technical issues in the direct conversion of CO_2 into value-added products, they are still promising for this reaction to mitigate CO_2 concentration in the atmosphere. In the last several years, intensive efforts have been made to study Cu-based catalysts, and substantial progress has been achieved in understanding their active sites and the reaction mechanism. This review discusses the structure and nature of active sites of Cu-based catalysts for CO_2 valorization in thermo-, photo-, and electro-catalysis. We present the characterization results of different types of Cu-based catalysts applied in these processes, unravel their active sites and structures, and figure out the most important and critical factors that drive the reactions on the sites. The principle and applications of various characterization techniques are also briefly analyzed and compared. It is expected to provide fundamental insights and perspectives for designing highly active and efficient catalysts for CO_2 conversion.

Keywords: CO_2 Conversion, Catalyst Characterization, Cu-Based Catalyst, Reaction Mechanism

1. Introduction

While utilizing fossil fuels through various industrial processes to generate energy and chemicals, it also emits carbon dioxide (CO_2), which has been recognized as one of the key greenhouse gases that result in the earth warmer than normal, causing imbalance and unsettling the ecosystem [1]. Human activities release an estimated 37.1 billion tons of CO_2 into the air each year, and about 80% of this amount is emitted directly from fossil fuels exploitation [2]. The increasing CO_2 concentration in the atmosphere will remain for the next few decades because fossil fuels will continue to be the primary source of energy [2]. The concentration is predicted to reach 550 ppm by 2050 [3, 4] and 590 by 2100 [5] if no proper measures are implemented. This continuous rise in CO_2 concentration in the atmosphere is a big challenge to mitigating global warming, raising serious concern and calling for solutions.

Carbon capture, storage, and utilization are proven strategies for controlling anthropogenic CO_2 emissions [6, 7]. The latter is pursued because of the possibilities of transforming the captured CO_2 into economically viable products like feedstocks for industrial processes. The economic benefit of converting CO_2 into chemicals and fuels is enormous. It helps in the net reduction of CO_2 emission, contributing to global emission control and decreasing dependency on fossil energy [8, 9]. Figure 1 shows how far CO_2 conversion technology has developed. The past few decades have seen substantial growth in research devoted to technologies for converting CO_2 into chemical products such as hydrocarbons and methanol by direct or indirect routes.

Efforts were much dedicated to the development of catalysts with high conversion, selectivity, and stability. An example is the methanol synthesis catalyst which is still suffering from low equilibrium concentration under high temperature and pressure operating conditions [10]. Most early CO_2 conversion technologies have undergone major or marginal changes to the current status that have improved the process even further, paved the way for possible future improvements. However, many proposed technologies are still at the infant stage and require significant improvement to be on course to an industrial scale implementation. The catalysts developed in the past have been optimized to high selectivity and stability. But issues bothering on recyclability and rapid deactivation by coking under harsh reaction conditions remain.

The captured CO_2 may be converted into fuels, construction materials, precursor chemicals for industrial products, such as fertilizers, plastics, adhesives, pharmaceuticals, and specialty chemicals like urea and salicylic acid [11]. For example, CO_2 can be converted into CO via the reverse water gas shift (RWGS) reaction and then hydrocarbons through the Fischer–Tropsch (FT) synthesis. CO_2 reformation of methane from natural or shale gas to produce syngas is also a well-established technology [12]. The syngas is a key starting material or feedstock of the present chemical industries. The direct conversion of CO_2 to methanol is still far from full maturity and profitable large-scale utilization. Also, enormous advances have been made in the catalytic conversion of CO_2 into short-chain products like lower olefins (C_2–C_4) [13]. However, it is still a far reach from achieving the selective conversion into long-chain hydrocarbons (C_{5+}). Although highly active and selective catalysts for some of these reactions are available commercially, the rapid loss of their activities under the harsh reaction conditions due to deactivation of the catalytically active components by sintering and coke deposition is challenging [14, 15]. The future holds even more opportunities for CO_2 conversion to other valuable materials. It has been found that striking CO_2 against an inert surface like Au foil can split the molecule to form molecular oxygen (O_2) and atomic carbon (C); the O_2 has many applications, such as in oxidation reactions. Oxygen is also safe as artificial air for astronauts traveling to and from space or other planets. This discovery is an inspiration to the Caltech reactor, which is proposed as a future reactor for removing CO_2 from the atmosphere.

Generally, methods, including thermo-, photo-, electro-catalytic reduction processes, and the combination thereof, have been adopted for CO_2 conversion [16-25]. The CO_2 reduction with H_2 gas, which can be obtained from the splitting/electrolysis of water or renewable energy sources, is a practical process for producing methanol using Cu-based catalysts, with demonstrations even at the commercial scale [10]. Numerous and extensive investigations have been conducted to synthesize, optimize, and develop catalysts to convert CO_2 to methane, methanol, ethanol, ethylene, and platform chemicals [26-29]. In many of the published studies, catalysts based on Cu nanoparticles (Cu NPs) have been found as the most active for CO_2 utilization by the reduction process [10, 30]. These are often supported catalysts that have interaction amongst the various components [31]. Although studies have provided particular understandings into the working states of the catalysts, challenges associating with the accurate characterization of the complex system make the findings lacking and studies inconclusive. Thus, the particular structure and active site of this type of catalysts are not fully understood. The accurate mapping of the activity-structure relationships of heterogeneous catalysts requires adequate knowledge of the structure and active sites/phases. Clear identification of the catalyst structures remains a major challenge and requires an extensive and thorough characterization to clarify the fundamental bulk and surface chemistries. The basic understanding of catalysis of CO_2 reduction with Cu can be attained if the structure and active surface of Cu-based catalysts are determined.

This review discusses the structure and active sites of Cu-based catalysts investigated for converting CO_2 to value-added chemicals. A brief overview of the most important and commonly applied techniques for characterizing catalyst structure and active sites is also presented. We highlights primarily recent works applying a handful of both common and advanced techniques for unraveling the possible active sites, providing a holistic discussion to elucidate the influence of the structure and active sites on the mechanism of the CO_2 reduction over Cu-based catalysts. Providing a general insight into this is crucial for improving the performance of the Cu catalyst systems and gaining a fundamental understanding of their activity.

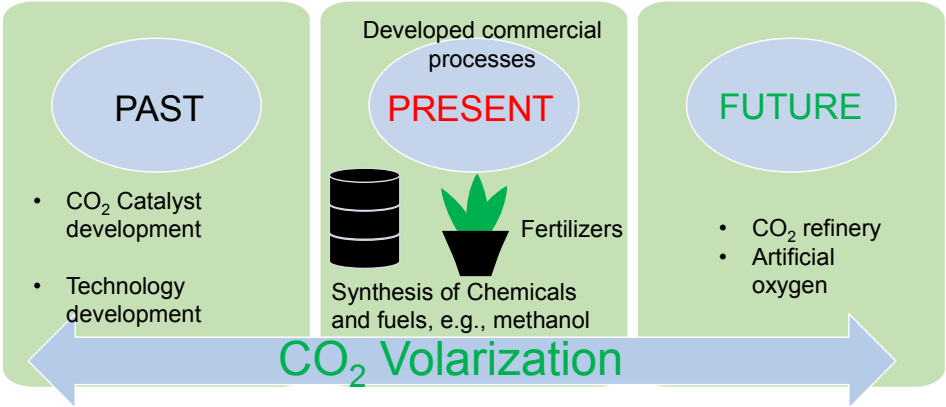

Figure 1. *The status of CO_2 volarization process.*

2. Catalytic Reduction of CO_2 to Value-Added Products

2.1. Thermocatalytic CO_2 Reduction

The thermocatalytic process of CO_2 conversion is performed at high temperatures in the presence of a heterogeneous catalyst. This process has a fast reaction rate with high efficiency, allowing production at high volume for industrial application [22]. It is of advantage over other processes for CO_2 conversion because of its more favorable kinetics. However, thermodynamics is a big issue. Different thermocatalytic reactions for CO_2 conversion are governed by different thermodynamics. Some reactions are endothermic, while some exothermic (Eqs. 1– 4). The thermocatalytic CO_2 conversion into fuels and chemicals requires a source of H_2, unlike the case of the electrocatalytic or photocatalytic process, where water is the preferred co-reactant. H_2 can be produced using renewable energy resources such as solar lights, wind, or hydropower. This process produces renewable fuels which can be stored and transported more efficiently. CO_2 can be hydrogenated to hydrocarbons via a combined RWGS and FT synthesis reactions route where in syngas (H_2 + CO) is first generated by the RWGS reaction followed by the subsequently hydrogenation of CO to hydrocarbon via FT synthesis. However, it is preferred to convert CO_2 directly into fuels and chemicals like methanol through hydrogenation. Another route for CO_2 hydrogenation is methanation, also known as the "Sabatier reaction," which produces synthetic CH_4. Thermocatalytic hydrogenation is also an important route for producing dimethyl ether (DME), higher alcohols and C_{2+} hydrocarbons. Nevertheless, this reaction is difficult because of the thermally stable nature of CO_2 molecule, resulting in low conversions. Because the catalysts for different products are different, we will be focusing only on reactions feasible over the Cu-based catalysts.

$$CO_2 + CH_4 \leftrightarrow 2CO + 2H_2 \quad \Delta H_{298} = 247.3 \text{ kJmol}^{-1} \quad (1)$$

$$CO_2 + H_2 \leftrightarrow CO + H_2O \quad \Delta H_{298} = 42.2 \text{ kJmol}^{-1} \quad (2)$$

$$CO_2 + 3H_2 \leftrightarrow CH_3OH + H_2O \quad \Delta H_{298} = -49.2 \text{ kJmol}^{-1} \quad (3)$$

$$CO_2 + 4H_2 \leftrightarrow CH_4 + 2H_2O \quad \Delta H_{298} = -164.9 \text{ kJmol}^{-1} \quad (4)$$

2.1.1. Cu-Based Catalysts for Thermocatalytic Reduction of CO_2

Most industrial-scale thermocatalytic processes proceed on catalysts based on Ni, Co, Cu, Cr, and Fe. Before choosing an active catalyst for a particular process, certain factors must be put into consideration. First, the CO_2 molecule is very difficult to activate; thus, a catalyst with high catalytic activity is needed. The commercially available methanol synthesis catalysts are inefficient for the direct CO_2 conversion to methanol because high methanol yield cannot be obtained in excess steam, which is also a reaction product in this process. The released amount of water drives the equilibrium in the opposite direction, towards CO_2 formation, resulting in low CO_2 conversions. Since the direct hydrogenation of CO_2 is much more attractive, a superior activity catalyst is therefore critical. Heterogeneous catalysts based on Cu have been demonstrated to be of superior activity in the direct conversion of CO_2 to fuels and chemicals such as methanol and CO.

Modified or supported Cu are very promising candidates for this process; however, suitable support is essential for the dispersion and stabilization of the active phase [32]. Cu/ZnO catalyst and its modified form are projected as the best for the CO_2 conversion into liquid chemicals (e.g., methanol). The ZnO in this catalyst can improve the dispersion and stabilization of Cu NPs. Cu/ZnO modified with Al_2O_3 is found as the active catalyst for the direct CO_2 hydrogenation to methanol even at the industrial level. The process is sustainable and green as the sources of hydrogen will not be depleted, and the methanol obtained from this could be referred to as "a renewable fuel." However, the catalyst is prone to deactivation by sintering of the Cu NPs at the high temperature (220–300°C) of operation. Other transition metals/metal oxides have been incorporated into the Cu/ZnO catalyst in the place of Al_2O_3. ZrO_2, Ga_2O_3, CeO_2 or In_2O_3 as support or modifier for bare Cu or Cu/ZnO have all exhibited good performance in the synthesis of methanol and formate from CO_2. Furthermore, the transition metals can combine with Cu to form bi-or-multimetallic catalysts. Their synergistic interaction with Cu can improve the activity. For instance, Zn-decorated Cu is a better catalyst than the pure Cu model catalysts [33]. Several studies have attempted to elucidate the active site structure of the Cu/ZnO-based and other Cu-based catalysts for methanol synthesis. The results revealed researchers remain conclusively divided on the relationship of the active species with catalytic performance. While some hold that the activity of metallic Cu was linearly related to the Cu surface area [10, 33], others note the catalytic activity, though related to the Cu surface area, largely deviate from linearity. However, both Cu^+ and Cu^0 species are believed to participate in the activity of Cu-based catalysts [34, 35], and a proper mix of Cu^0 and Cu^+ in a single system is crucial for the catalytic performance in CO_2 to methanol conversion [10, 36, 37]. In a reduced catalyst, Cu was found to exist in its metallic form [38]. The absence of Cu^0 species in a catalyst sample as confirmed by XRD and TPR reflected in the lack of activity in the CO_2 hydrogenation to methanol [41]. Other studies observed active sites as isolated Cu^+ ions in the ZnO matrix, Cu^+ species stabilized by Cu–Zn alloys, the Cu/ZnO interface, Cu clusters or strained Cu particles [39, 40]. In all, these catalysts are characterized by well-defined active sites where reactions occur.

2.1.2. Mechanism of Thermocatalytic Reduction of CO_2

Mechanistic studies have been at the center of the thermocatalytic CO_2 conversion research. Several review articles have identified the mechanism of some reactions, such as CO_2 to methanol [42-45]. Two mechanisms have been

extensively discussed for the Cu catalyzed hydrogenation of CO_2 into methanol [43-47]. One of the pathways produces CO intermediate generated from RWGS: $CO_2 + H_2 \rightarrow CO + H_2O$ reaction via carboxyl ($^*HOCO$) that subsequently hydrogenates to CH_3OH. The other pathway passes through the key intermediates of formate ($^*HCOO$), dioxomethylene ($^*H_2COO$), formaldehyde ($^*H_2CO$) and methoxy ($^*H_3CO$) to the final product, CH_3OH. Still, other pathways have been proposed (Figure 2). The modified formate pathway produces $^*HCOO$, which is hydrogenated into formic acid ($^*HCOOH$) and through other intermediates to CH_3OH. CO_2 can dissociate and hydrogenate via $^*HCO$, $^*H_2CO$ and $^*H_3CO$ intermediates to CH_3OH. In the presence of steam, the water-mediated mechanism can occur, where the $^*HOCO$ intermediate is involved also. In this mechanism, water serves as the source of H atom, and the $^*HOCO$ intermediate is further hydrogenated to dihydrocarbene ($^*COHOH$), leading to the formation of COH, and CH_3OH [48]. Generally, under conditions typical of the industrial methanol synthesis from CO_2 hydrogenation, the following intermediate species have been identified: $^*HCOO$, $^*HCOOH$, $^*CH_3O_2$, $^*CH_2O$, and $^*CH_3O$ [43, 49]. Over the industrial $Cu/ZnO/Al_2O_3$ catalyst, FTIR spectroscopy measurement revealed that hydrogenation of both formate and methoxy species was the rate-determining step [10, 42]. When CO_2 was used as the feed, formate was the dominant species, but methoxy species predominantly appeared with CO as the main reactant.

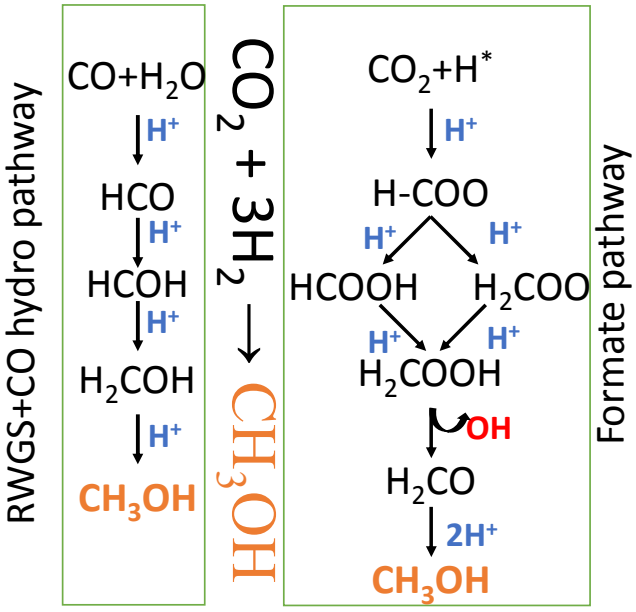

Figure 2. *Simplified mechanism for CO_2 hydrogenation to methanol.*

2.2. Photocatalytic CO_2 Reduction

Interests in the photochemical reduction of CO_2 sprung up following the pioneering work of Inoue et al. [50] in the late 1970s. Also called artificial photosynthesis, the photocatalytic reduction of CO_2 with H_2O using solar energy is an attractive route for transforming CO_2 into high-value products, although molecular H_2 can also be used [51-54]. Solar energy (light) plays a crucial role in this reaction by inducing charge excitation. The photocatalyst must possess the ability to absorb light and generate electron-hole pairs that are then separated and transferred to the surface of the catalyst surface to take part in the reduction and oxidation half-reactions [55].

2.2.1. Cu-Based Catalysts for Photocatalytic Reduction of CO_2

The photocatalysts investigated for the reduction of CO_2 are mostly semiconductors, including TiO_2, ZnO, and CuO_x [56, 57], but our interest in the present work focuses on Cu-based semiconductors/photocatalysts. Cu can trap generated electrons, preventing the fast charge recombination. This function promotes the redistribution of charge on the surface of the photocatalysts which increases photoefficiency [30, 57, 58]. CuO and Cu_2O have been extensively studied in the photoreduction of CO_2 to valuable products, such as methanol, methane, formic acid, and CO [59-61]. Cu_2O is a p-type semiconductor with a wide bandgap of approximately 2.2 eV, which is very attractive as a photocatalyst for CO_2 reduction in the presence of visible light. However, Cu_2O has issues related to its stability as it can be easily oxidized or reduced by the photogenerated charge carriers [62, 63].

Generally, pure copper oxides exhibit a low selectivity for CO_2 reduction products due to fast charge recombination rates [64]. However, the selectivity can be improved by incorporating other materials as supports or using copper as a co-catalyst with other photocatalysts. As reported, Cu_2O with Al-doped ZnO and TiO_2 as protective layers improved the stability of Cu_2O for photo-electrochemical water splitting [65]. The photoactivity of Cu_2O was improved when used as a co-catalyst with TiO_2, carbon quantum dots (CQDs), RuO_x, or SiC [61, 66]. The improvement is generally a result of the cooperative effect between Cu particles and the co-catalyst, facilitating both trapping processes of photoexcited electrons and holes and decreasing the recombination rate [57]. CQDs and TiO_2, for example, possess excellent charge separation and transfer capabilities. On the other hand, Cu ions (Cu^0, Cu^+, Cu^{2+}) can improve the formation of sites for electron trapping and facilitate charge transfer when incorporated into TiO_2 [54, 66, 67].

Tian et al. [68] demonstrated the photocatalytic activity of $CuO/Cu_2O/Cu$ nanorods-decorated rGO composite under visible light irradiation. The rGO assisted in the electrons transfer from and within the $CuO/Cu_2O/Cu$ nanorods. Cu_2O/reduced graphene oxide (Cu_2O/RGO) junction composite synthesized by a microwave-assisted in situ reduction was found to increase the photoreduction activity for reducing CO_2 to CO by twofold. Activity results correlated with the retarded electron–hole recombination, efficient charge transfer (Figure 3 a, b), and protective function of RGO [60]. CuO readily redistributed electric charge on the surface of the semiconductor support and trapped electrons, preventing the recombination of electron-hole pair and increasing its photoefficiency in photo-reduction of CO_2 to methanol [69]. It was found that photocatalysts promoted by CuO performed better than the materials promoted by Cu^0 and

Cu^+ species [30, 70] as opposed to other studies where either Cu^0 or Cu^+ or both species were believed to drive the activity [71, 72]. It has also been suggested that during the photochemical reaction, Cu^+ species may be reduced by photogenerated electrons to Cu^0, which can trap electrons. However, Cu^0 can easily be re-oxidized to Cu^+ in the air.

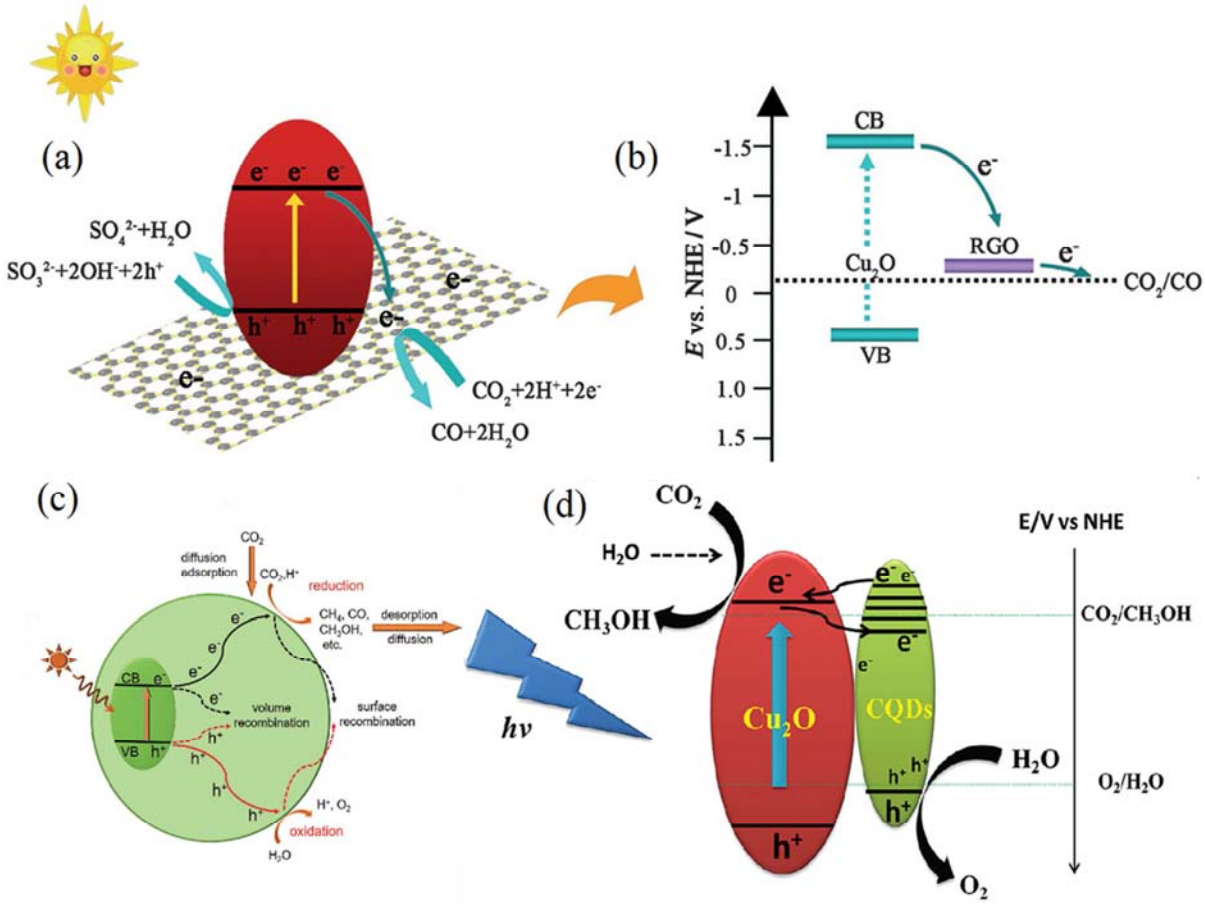

Figure 3. *(a), (b) Charge transfer processes in Cu_2O/RGO composites [60], (c) Schematic showing five fundamental steps in photocatalytic CO_2 reduction [73], (d) Proposed photocatalytic reduction mechanism of CO_2 catalyzed by CQDs/Cu_2O [61].*

2.2.2. Mechanism of Photocatalytic Reduction of CO_2

Typically, the heterogeneous photocatalytic process consists of five sequential steps –light absorption and excitation to generate electron and hole, charge separation, CO_2 adsorption, surface redox reaction, and product desorption [60, 74, 75] (Figure 3 c). The photocatalyst first absorbs the solar energy in a step known as the "light harvesting step". When incoming light illuminates the photocatalyst, electrons are excited from the valance band (VB) to the conduction band (CB), leaving an equivalent number of holes in VB [76, 77]. This process requires energy equivalent to or greater than that of the semiconductor catalyst's bandgap energy. However, photocatalysts cannot have a very large bandgap since this would limit their ability to use the solar spectrum effectively. The light-harvesting step depends on the morphology and structure of the catalyst used, and could be improved using meso- or microporous catalytic structures and band engineering [77]. The next step is the spatial separation of photo-generated electrons and holes involving excitation of the electrons in the valence band to the conductance band. This results in proton generation in the conduction band and holes in the valence band [78]. The excitation can be improved by tapering the band gap. The electrons tend to move toward the outer region of the semiconductor but can be restricted by the catalyst active sites present at the surface. The recombination of electrons and holes (volume) may take place. Thus, the process of charge separation is directly competing with the charge recombination. Generally, the recombination stages should be prevented because it causes energy loss [79]. The third step is CO_2 adsorption and reduction to the $CO_2^{\bullet-}$ radical anion. In this step, electrons must be transferred from the photocatalyst to the CO_2 molecule. Photocatalysts with large surface typically have more active sites for CO_2 adsorption. Furthermore, modification of the photocatalyst surface with alkali could improve the CO_2 adsorption, as in the case for TiO_2 [51, 75]. This is because the acidity of CO_2 molecules would promote the reaction between CO_2 and the alkalinic photocatalyst surface, resulting in intermediates generation and favouring CO_2 molecule activation and subsequent reduction. The surface redox reaction is the fourth stage, in which electrons and holes migrate to the surface, causing surface recombination. Both the oxidation and reduction

reactions are affected by the produced electrons and holes. The holes catalyze water oxidation to molecular O_2, while the electrons reduce CO_2 to different photocatalytic products [80, 81]. This step is followed by the final product desorption.

Some specific examples of the photoreduction mechanism of CO_2 to specific molecules are briefly discussed. In the formation of methane over (Au, Cu)/TiO_2 under visible light in the presence of H_2O, the reduction of CO_2 proceeds by adsorption of both reactants, CO_2 and H_2O, leading to the formation of surface adsorbed $CO_2^{\bullet-}$ species upon their activation by electron-hole transfer. This is swiftly followed by the cleavage of the C–O and formation of C–H bonds in a pathway termed "the carbine pathway" [82]. Li et al. [61] proposed a mechanism for reducing CO_2 to methanol under visible light over Cu_2O/CQDs. Electron-hole pairs are produced upon excitation of Cu_2O by visible light; the produced electrons are consumed for reducing CO_2 to methanol on the Cu_2O surface [61]. The holes transferred to the surface of CQDs, where they oxidize H_2O to O_2. White et al. [83] described a mechanism involving the proton transfer to an oxygen atom on $CO_2^{\bullet-}$ assisted by water, the loss of an OH group, and the subsequent second electron transfer to produce an adsorbed CO species as demonstrated in the reduction of CO_2 to formate on transition metals. The addition of a second electron also led to the formation of the formate ion [83]. The surface intermediates, particularly $CO_2^{\bullet-}$, Cu–CO, and carbon deposits on the surface, can be detected by surface-sensitive characterization tools, such as in-situ FTIR [82, 84]. Kang et al. [84] used in situ FTIR experiments to detect the surface species during the CO_2 reduction to CH_4. A series of adsorption bands around 1330–1590 cm^{-1} and 1600–1890 cm^{-1}, whose intensities increased with time appeared under the UV/Vis irradiation, attributed to the bending vibration of C–H in CH_4, and the stretching vibration of C=O and the asymmetric stretching of O–C=O bonds in the intermediate products, respectively, such as aldehydes, carboxylic acids, and bidentate carbonates [85].

2.3. Electrocatalytic CO_2 Reduction

The electrocatalytic reduction of CO_2 is an appealing method for CO_2 utilization [86]. This process is characterized by the generation of a wide spectrum of products through different reaction pathways or a combination of the pathways, depending on factors, such as the nature of catalyst, nature of electrode, electrode potential, electrolyte composition, pH, temperature, and CO_2 feed concentration, the configuration of the cell, and presence of adsorbents [87-90]. The electrode potential regulates the production of electrons-transported to the cathode, where they combine and reduce CO_2 to various products. Anode is where water oxidation reaction occurs. In the aqueous medium, if the electrons react with protons, hydrogen will be produced instead (hydrogen evolution). The products obtained from the electrochemical reaction can be made selective by changing the applied electrode potential and the catalyst. Certain products such as methanol and C_{2+} hydrocarbons, difficult to produce by the thermocatalytic process at low reaction temperatures and pressures, can be easily realized by the electrocatalytic process at near or ambient temperature. Furthermore, electrochemical cells for the reduction of CO_2 are easier to scale up.

Since the CO_2 electroreduction reaction is governed by unfavorable thermodynamics and low Faradic efficiency, high overpotential (high energy) is always required to form a product. The kinetics are too slow to form an energetically reaction intermediate, which can be stabilized by selecting a proper catalyst that can lower the high overpotential requirements for the product formation and selectivity [91]. Meanwhile, some products require higher overpotential than others. For example, methanol and methane that need multi-electron for their formation require higher overpotential than CO or formate which one- or two-electron transfer is sufficient for their formation [92]. Moreover, the solubility of CO_2 in the aqueous electrolyte is poor, which hinders the free mass transfer of CO_2 from the feed gas to the catalyst surface, resulting in the overall low current density and productivity.

Many studies on this process have been carried out in both the liquid and gaseous phases using various catalysts and electrolytes [92]. The design of efficient CO_2 reduction electrocatalysts/electrolytes needs a proper comprehension of the mechanisms through which products are formed during the reaction. Among the reduction products, the formation of C_1 products (e.g., CO and HCOOH) on the bulk catalyst surface follows a relatively simple pathway. In contrast, the mechanism of CO_2 reduction to C_{2+} products is a more complex process with many possible pathways involving both electrochemical and chemical steps [89, 92-95].

2.3.1. Cu-Based Materials for Electrocatalytic Reduction of CO_2

Copper has a unique ability to promote the selective reduction of CO_2 to different products like formic acid, methane, methanol, ethanol, CO, and for C-C coupling toward C_{2+} products with good Faradaic efficiencies when compared to other catalysts [94-99]. It has been reported that to date, only Cu catalyst can catalyze CO_2 reduction to substantial amounts of alcohols [96-98]. This may be associated with the adsorption energy of CO on Cu. Moderate or optimum adsorption energy is important because it allows the activation for further reduction and C-C bond formation, which is difficult to achieve with other metals that bind CO either too weakly or too strongly according to the Sabatier principle [8]. Cu has a CO adsorption strength close to the optimum, exhibits selectivity for various products from CO_2 reduction reaction. However, Cu catalysts often suffer from low conversion efficiency, poor selectivity, and unidentified intermediates [94]. To improve selectivity, the modification of the adsorption strength of CO on the catalytic sites is crucial [8]. Moreover, Cu catalysts perform at high overpotentials to attain substantial selectivity to C_{2+} products [98, 100].

The surface and its morphology plays a remarkable part in the selectivity of products. It was observed that the ratio of C_1 to C_2/C_3 products was highly influenced by the surface morphology of Cu [101, 102]. The open Cu (100) surface

exhibited greater selectivity to products with C-C bonds than the close-packed Cu (111) facet [94]. Thus, identifying the possible mechanisms for the CO_2 reduction reaction remains a continuously interesting topic. Polycrystalline Cu is selective to CO, HCOOH, $HCOO^-$, H_2, and CH_4 at potentials more reductive than −0.8 V vs. RHE, while (110) and (111) steps nearby (100) terraces are selective toward C_{2+} products [103]. This could influence the elementary steps that control the product distribution [94].

2.3.2. Mechanism of Electrocatalytic Reduction of CO_2

Based on experimental data and density functional theory calculations, comprehensive mechanisms for CO_2 reduction on Cu electrocatalysts have been discussed. CO_2 is first chemisorbed, then reduces to adsorbed formate intermediates ($HCOO^*$), which eventually desorbs as formate ions. On the other hand, the $^*COOH$ intermediate, which is adsorbed via its C atom, would be converted to $^*CO$ intermediate. $^*CO$ is the key intermediate in the formation of hydrocarbons and alcohols [92]. Generally, it has been proposed and somewhat accepted that $^*CO$ is a key intermediate in the formation of hydrocarbons; however, a conclusive mechanistic view of Cu driven electroreduction of CO_2 to multi-carbon products is still far from reach due to the complexity of the involved reactions [98, 104]. Understanding the detailed mechanisms for forming C_1 and C_2 has been pursued by several research groups in isolation and collaboratively.

Hori, one of the pioneer discoverers of Cu as a catalyst in the electrochemical CO_2 reduction to CO, proposed that, in the aqueous medium, CO_2 initially adsorbs on the surface of electrodes and forms carboxyl intermediate ($^*COOH$) via the formation of a CO_2 radical (CO_2^*) from which CO is produced when CO_2^* is strongly adsorbed and stabilized; weakly adsorbed or free CO_2^* leads to the formation of $HCOO^*$ [93]. Recent studies based on DFT calculations proposed the formation of $^*COOH$ through a proton-electron transfer to CO_2 [92, 105]. The electroreduction of CO_2 to methane follows the CO-mediated reaction pathway, involving the protonation of CO and the C–O bond scission in successive steps, formation of $^*CH$ species, and finally CH_4 by the proton-electron transfer process [106]. However, there is a disagreement about the intermediary CH_4 precursor. Hori [89] suggested a hypothetical intermediate $^*COH$ is the precursor to CH_4, whereas, $^*CHO$ intermediate is found in more recent studies [94, 106]. The CO_2 electrolytic reduction to methanol follows a similar reaction pathway to that of methane, involving the adsorption of formed CO and formation of $^*CH_2OH$ species. This species then produces methanol via proton-electron transfers. Generally, in the formation of C_1 products, the conversion of CO_2 to CO precedes the adsorption of CO on the Cu surface which is considered as the first reaction step in many theoretical studies [94].

The electroreduction mechanisms of CO_2 into multicarbon products are more complex. Reaction pathways to C_{2+} products, especially ethylene and $C_{2+}OH$, have been widely studied, and several mechanisms have been proposed [94, 107-109]. One of the mechanisms, according to Koper and co-workers, follows the CO dimerization pathway, in which the rate-determining step is the coupling of two CO molecules mediated by electron transfer to form $^*C_2O_4$. Subsequently, this dimer is transformed into C_2O_4 and EtOH by proton-electron transfer [107]. Based on this, Cheng et al. [108] devised a more complete mechanism in which hydrogenation of an oxygen atom ($^*COCO+H \rightarrow {}^*COCOH$) follows CO dimerization. However, using the CEP model, Goodpaster et al. [109] found that the reduction of CO to $^*CHO$ followed by reaction with $^*CO$ to generate $^*COCHO$ was preferred to $^*CO$ dimerization and subsequent reduction at high potentials. A closely related mechanism was reported by Bell and co-workers [94]. The adsorbate CO is firstly hydrogenated to $^*CHO$ intermediate, and subsequently couples with another CO molecule to form $^*COCHO$. In this pathway, the C-C bond is formed, and various products (e.g., ethylene, ethyl alcohol, and aldehyde) are produced via proton-electron transfers. Over Cu (100) surface, at –1 V with reference to the RHE, the first reaction step was the CO adsorption of the surface with a good binding strength due to charge donation from the surface to the empty π^* orbital of CO. This was followed by the C-C bond formation via the following reactions to $^*COCHO$, $^*CO+H \rightarrow {}^*CHO$ and $^*CHO+CO \rightarrow {}^*COCHO$ (Figure 4) [94]. Lin et al. [95], by computational method, explored the mechanistic steps in ethanol formation on the Cu-Cu(I) ensembles and found the various hydrogenated intermediates to start from the hydrogenation step of the $^*CCO$ generated from the dehydration step of the observed $^*OCCOH$ intermediate.

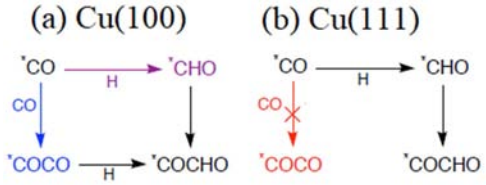

Figure 4. *Formation of C-C bond and $^*COCHO$ on Cu (100) and Cu (111).*

The pH influence on the reaction mechanism has also been demonstrated and discussed, and variation in the pH of the system could lead to the formation of a different product [109-111]. The fact that ethylene formation is pH-dependent on a RHE scale implies that the rate-determining step proceeds in without a proton [111]. Also, that C-C bond formation is the rate determining step via the $^*CO \rightarrow {}^*CHO \rightarrow {}^*COCHO$ pathway justifies the observed pH dependence [109]. For the combined pathway of CO dimerization followed by reduction to $^*COCOH$ ($^*CO \rightarrow {}^*COCO \rightarrow {}^*COCOH$), the C-C coupling step is the rate-determining step, too, because the reaction is also pH sensitive. This is also the case if the $^*CO \rightarrow {}^*COH \rightarrow {}^*COCOH$ sequence is considered [110]. Therefore, the combined evidence suggests the existence of pH-sensitive mechanisms for C-C bond formation on Cu.

Cheng et al. [108, 112, 113], using full solvent quantum mechanics molecular dynamics, studied the mechanism and identified the reaction intermediates during the operando electrocatalytic CO_2 reduction to CO. It was predicted that the

reaction involves physisorbed CO_2 (*l*-CO_2), chemisorbed CO_2 (*b*-CO_2), formation of *COOH, and *CO at pH 7 [113]. The characteristic peaks listed in Table 1 are IR active but Raman inactive. The spectroscopy of CO_2 reduction to CO reported from experimental investigations exhibited debated peaks assignment; however, the *b*-CO_2, *COOH, and $^*CO_3^{2-}$ all exhibited comparable spectroscopy fingerprint signals at 1400 cm^{-1}, difficult to distinguish them [114-117]. The possible reaction intermediates and products of electrochemical reduction of CO_2 on Cu electrode were studied using in situ ATR-SEIRAS and isotopic labeling [118]. Results found that formate and carbonate, such as bidentate species, were formed at negative potential. The more negative potential shifted the selectivity towards CO and bicarbonate. The formation of CO became significant upon the appearance of the CO_2 dimer radical anion by disproportionation reaction. Adsorption of CO was restricted to -1.4 V, below which no significant adsorption was feasible; only residual bi-carbonate was present. One issue with this characterization technique is the transient nature of some species, which might escape measurement due to their short lifetimes.

Table 1. *Intermediates and their spectroscopic signature during CO_2 conversion to CO, C_2H_4 and C_2H_5OH on Cu(100) surface at 298 K. Data extracted from ref. [112, 113].*

CO							
Adsorbed species	*l*-CO_2	*b*-CO_2	*COOH	*CO	$^*CO_3^{2-}$		
IR frequency (cm^{-1})	1330	1365, 1397	1420, 1287	1790, 2050-2100	1720, 986		
Functional group	O=C=O	C=O	C=O, C-OH	C=O	C=O, C–O		
Vibration mode	symmetrical	stretch	stretch	in plane-bend	stretch		
C_2H_4 and C_2H_5OH							
Adsorbed species	OC-CO	*OC-COH	*HOC-COH	*C-COH	*CH-COH	*C-CH	*C-CH_2
IR frequency (cm^{-1})	1171	1231, 1360	1439, 1,324, 1,187	1609	1422, 1251	1559	1,451, 1,320
Functional group	C-O^-	H-O-C, C=O	C=C, H-O-C=C-O-H, C-OH	C=C	C=C, C-OH	C=C	C=C
Vibration mode		in-plane bend, stretch	stretch, symmetric in-plane bend	stretch	stretch	stretch	stretch

2050-2100 cm^{-1} refers to C=O stretch in adsorption on the bridge site.

3. Cu-Based Catalysts for CO_2 Conversion to Chemicals and Fuels

3.1. Types of Cu-Based Catalysts

The most selective catalytic materials for this process are based on Cu. Several Cu-based catalysts have been investigated for the direct or indirect transformation of CO_2 to important chemicals and fuels [119]. In our previous review [10], we discussed Cu-based catalysts for the CO_2 reduction to methanol. Cu catalysts in the modified or supported form are very efficient for methanol synthesis in the thermocatalytic process. In this follow-up work on determining the structure and active sites of these catalysts, we briefly discuss different kinds of Cu catalysts applied in converting CO_2 by different processes discussed in the previous sections. The Cu-based catalysts can be roughly classified into four types: (i) Cu/CuO_x nanoparticles, (ii) supported Cu catalysts, (iii) Cu bimetallic and multimetallic systems, and (iv) oxide-derived Cu (OD-Cu) catalysts [120].

Cu/CuO_x NPs are synthesized mostly by chemical, photochemical, electrochemical, sonochemical and thermal synthesis methods [119, 121, 122]. Pure Cu NPs can be prepared by the chemical method on inert support that has no contribution to the intrinsic activity of the catalyst or interaction with the active Cu (e.g., SiO_2) [123]. Very small Cu NPs with a narrow size range often result when a higher Cu loading is placed on the active supports. Cu NPs and the corresponding bulk materials exhibit different activities because of their differences in size and shape. They typically perform CO_2 reduction by different processes; however, their activity is depended on the particular process adopted. The use of pure Cu NPs is limited by their intrinsic instability under atmospheric conditions and ability to oxidize easily. Cu_2O NPs of different morphologies can similarly be prepared by the chemical method via the dissolution of Cu precursors at a low temperature in the presence of structure-directing agents [124]. Such oxidic catalysts have pronounced activity in photoreduction reactions. This type of catalyst is unstable in this reaction; however, using suitable supports, such as carbon materials, can remarkably improve the stability.

(ii) Supported Cu catalysts. Cu NPs sit on active supports exhibit superior properties compared to the bare Cu NPs, partly due to the increased stability of the particles by tuning their sensitivity to physical and chemical conditions such as oxygen, water, and other chemical entities. This, in particular, has enabled tailoring the properties of NPs in general toward specific applications. Several materials are useful as supports for Cu catalysts. They include carbon materials, metal oxides (e.g., ZrO_2 and Ga_2O_3), polymer materials, silica, zeolites, etc. [99]. This support can combine with the active metal to form interfaces highly active as sites selective to a product. For instance, over the Cu/ZrO_2 catalyst for CO_2 conversion, in which ZrO_2 is the support, the formation of both CO and CH_3OH occurred on the surface and Cu-ZrO_2 interface, respectively [123]. Cu NPs can also be supported on an oxide of Cu (CuO_x) to tune the selectivity of the product. For example, the deposition of metallic Cu NPs on Cu_2O films was demonstrated to change the product selectivity from gaseous products to CH_3OH on the Cu/Cu_2O interface in the photocatalytic conversation of CO_2 to methanol in aqueous solution [128]. The Cu/Cu_2O interface can be adjusted by loading different masses of Cu on the Cu_2O layer and allowing

it to evaporate. Cu_2O supported on reduced graphene oxide, prepared by a one-step micro-waved assisted chemical method, showed enhanced activity for the photoreduction of CO_2 when compared with an optimized bare Cu_2O or that supported on RuO_x [60]. The improved catalytic activity is attributed to the efficient charge separation and transfer and the stability and protection offered by the reduced graphene oxide.

(iii) While the interaction between metal NPs and support may be restricted to the surface, some metals can combined with Cu to form multimetallic systems such as alloys [125, 126] and intermetallics [127]. These systems differ from supporting materials because the foreign element can penetrate the lattices of the base metal, altering the electronic and geometric properties. Such materials often exhibit unusually high activity, physical and chemical properties, and thermal stability.

(iv) Oxide-derived Cu (OD-Cu), generally denoted as CuO_x/Cu, is a group of Cu-based catalysts that can be obtained by a variety of methods, including oxidation of Cu foils or films, electrochemical reduction of copper oxides, and oxidation-reduction treatment of Cu [128-131]. For example, the synthesis of Cu_2O-derived Cu was achieved through the electrochemical reduction of Cu_2O on carbon paper substrate [132, 133]. According to XRD data, the Cu_2O films exhibited predominantly (111) facet but largely retained their morphology with rough surface and cracks at grain boundaries. The OD-Cu catalyst is often associated with changes in morphologies compared to its precursor metal/oxide, which benefits its performance [134]. Mostly utilized in the electrochemical reduction of CO_2, the OD-Cu catalysts show an overall higher activity for producing C_{2+} products such as ethylene and ethanol at lower overpotentials than Cu NPs and have high Faradaic efficiency (FE) for CO reduction [90, 96, 128, 134-136]. The former is due to the presence of residual oxygen, which is debated in the literature [137]. Although the OD-Cu catalyst exhibits better FE for reducing CO to alcohols, it is more difficult to effectively and directly reduce CO_2 to products than CO and formate. The formation of heavy carbon products would proceed through subsequent CO and/or formate reduction [138]. Zhuang et al. [139] synthesized and characterized an OD-Cu catalyst for the electroreduction of CO to C_3 alcohol fuels. The Cu_2O NPs were first formed via the nucleation and growth of nanocrystals, followed by a mild acidic etching that resulted in the formation of Cu_2O particles with open morphology [140]. The obtained Cu_2O particles were deposited onto a carbon substrate and the final nano-hollow Cu catalyst was produced via an in situ CO electrochemical reduction. Another Cu material with comparable with but simpler chemistry that the OD-Cu is the polycrystalline Cu (129, 130). This material is often used as working electrodes in the electroreduction process. It exhibited a good activity and selectivity for CO reduction at low potentials in KOH solution [141]. Generally, Cu electrocatalysts form highly reduced products from CO_2 and more selective to C_{2+} due to their intermediate binding of CO [142].

3.2. Catalyst Structures

3.2.1. The Nature and Structure of Active Sites

In any catalytic reaction, the catalyst employed should have appropriate activity, selectivity, stability, and be affordable, mainly depending on the kind of active sites it has.

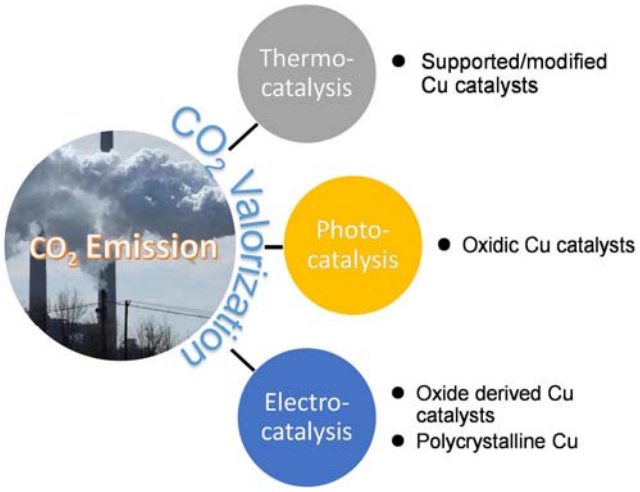

Figure 5. *Most active types of Cu catalyst for CO_2 reduction.*

For heterogeneous catalysts, active sites could be referred to as atoms, ensemble of atoms, crystal faces or areas on the catalyst surface that directly catalyze a reaction [103, 143, 144]. In regard to CO_2 reduction, the active sites must be characterized by the ability to activate CO_2 and form bonds to yield product precursors or intermediates. Moreover, the active sites should not be too active for dissociating H_2 into atomic adsorbed H^* [145].

Different Cu catalysts possess different active sites. Cu NPs present Cu species as active sites for hydrogenation of CO_2 to chemicals [146]. Recent experimental investigations have shown the Cu NPs are active in converting CO_2 and CO to alcohols [147, 148]. In particular, the grain boundaries of the NPs resulted in excellent catalytic performance. Typically, the $^*OCCOH$ intermediate formation was feasible on the sites with an under-coordinated surface near a subsurface stacking fault according to the multiscale simulation method [147]. The under-coordinated sites are more active than the low index surface, such as facet, edge, or corner sites in CO_2 electroreduction [149].

Combination of Cu with another metal and/or metal oxides proves an invaluable strategy to enhance the effectiveness of the active sites [146]. The Cu NPs supported on active support materials can exhibit different active sites from the pure NPs or that supported on an inert support. For example, the active sites of Cu/ZnO-based catalysts explored in the CO_2 to methanol synthesis have been a subject of interesting discussion. It has been proposed that the Cu-Zn interface, Cu-Zn bimetallic surface, Cu-Zn alloy or Zn decorated in Cu are all active for CO_2 conversion. The possible active sites or structures of some Cu-based catalysts are discussed subsequently. How the interfacial contact between Cu and

ZnO is constituted is an important factor that determines the character of the active site [125]. The OD-Cu catalyst reduces to metallic Cu during electrochemical reduction of CO_2 [150]. Moreover, CuO_x exists on the catalyst surface and responsible for the adsorption of $^*CO_2$ and OCO^- species. The oxide species is crucial in activating CO_2 and in C–C coupling according to studies using ambient-pressure X-ray photoelectron spectroscopy (AP-XPS) and electron energy-loss spectroscopy (EELS) [150, 151]. Each of these active sites plays defining role in the overall reduction process.

One of the fundamental hindrances in developing a rational design protocol for the CO_2 reduction catalysts, as observed in most heterogeneous catalysts, is the complexity of the resulting catalyst system that complicates the detailed characterization of their active sites [125]. Thus, a proper identification of the structure and composition of the active site is essential for comprehension and improvement of catalyst properties [152-154]. Generally, the real active sites of the Cu-based catalysts for CO_2 conversion remain a heated topic of discussion in the literature with catalytic activity attributed mainly to Cu^0, Cu^+ or both species and Cu-metal/metal oxide interface [10, 33, 155, 156]. For example, different types of active sites exist on the conventional ($Cu/ZnO/Al_2O_3$) methanol synthesis catalyst: the Cu–Zn interface, metallic Cu sites, and ZnO exposed sites [157-159]. Moreover, the composition of the different chemical state of Cu, which most times are the active sites, can vary. As reported, the composition of Cu^{2+} and Cu^+ during CO_2 transformation varied over a range depending on factors such as synthesis method, presence of promoter and matrix, and extent of reduction [160].

The complexity of the nature of active sites will be increased due to the synergistic interaction between the support and metallic Cu particles [161]. Synergy can result in the formation of new active sites [36, 162-164]. For example, the addition of ZrO_2 to Cu/ZnO catalyst promoted a new Cu phase formation as observed by H_2-TPR experiments [36]. In addition to Cu^+ that formed upon reduction of the catalyst, a peak that emerged at about 423 K indicated the formation of a new CuO phase, which is thought to result from the dissolution of zirconium ions in the copper oxide phase. From both experimental and theoretical investigations of ZnCu and ZnO/Cu model systems, surface oxidation of ZnCu occurred under the reaction conditions such that Zn on the surface transformed into ZnO, allowing ZnCu to attain the activity of ZnO/Cu with the same Zn coverage [164]. It demonstrates the importance of the synergistic interaction of Cu and ZnO at the interface that facilitates methanol synthesis.

The synthesis of methanol by Cu NPs can be promoted by ZnO. It has been demonstrated from both experimental and theoretical calculations that Zn atoms migration in the Cu surface promotes methanol synthesis [163]. The methanol synthesis activity was found to be highly dependent on Zn coverage, which was determined to relate to the reaction conditions and size of Cu and ZnO NPs (Figure 6). Thus, the size-dependent activities of NPs reveal that a synthesis strategy that can regulation the size of NPs can be adopted to design synergetic functionality in binary NP systems.

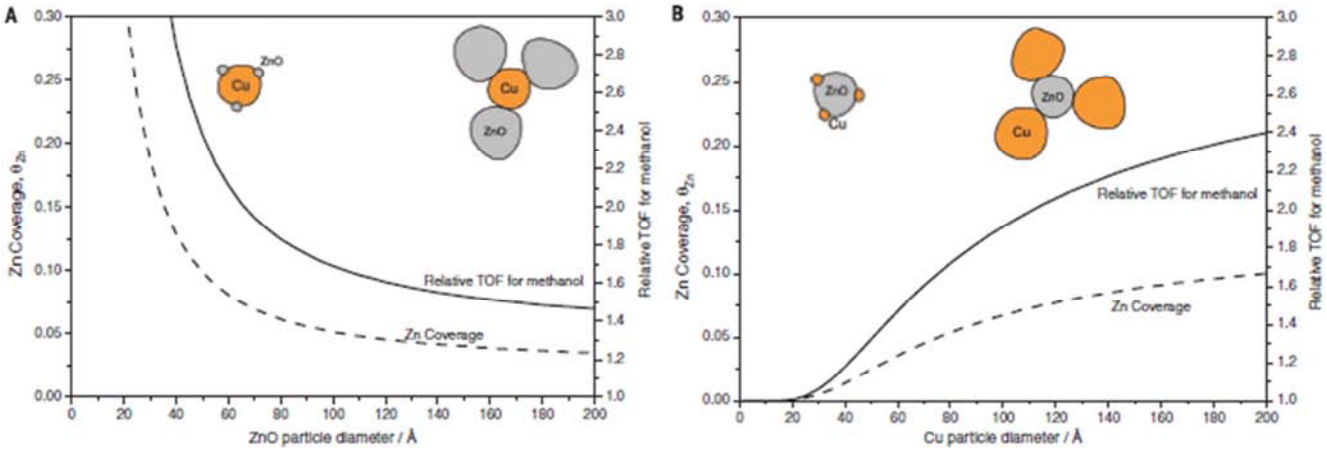

Figure 6. *(a) Modeling of Zn coverages of Cu NPs and (b) relative methanol turnover numbers of the $Cu/ZnO/Al_2O_3$ catalyst as a function of ZnO and Cu particle sizes [163].*

The chemical and structural changes of Cu catalysts may affect their stability and selectivity toward certain reaction products while identifying the catalyst active sites provides insights into the mechanisms of the catalytic processes. Generally, Cu-based catalysts present three major active sites for CO_2 reduction reactions, besides other specific sites reported in the literature. The results of detailed theoretical and experimental investigations on these active sites using state-of-the-art characterization techniques are discussed. [152, 165-167].

3.2.2. Functions of Various Cu Species at different Oxidation States

(i) Metallic Cu

Metallic Cu (Cu^0) plays a fundamental role in the adsorption and activation of H_2, which spills over to the support, providing H atoms to form intermediates. Metallic Cu sites adsorbed and dissociated H_2 into adsorbed H^* atoms for reaction with adsorbed CO_2 at adjacent In_2O_3 sites on a

Cu-In-Zr-O catalyst [162]. Cu^0 was found to be the active site on single crystal Cu (100), Cu (110), and polycrystalline Cu films with exposed Cu (111) facets [161, 168, 169]. From the HRTEM image of reduced Cu-In catalysts on zirconia that clearly marked the formation of three different phases with lattice corresponding to the (111), (111) and (011) planes of Cu^0, CuO and ZrO_2, the subsequent mechanistic study identified Cu^0 was active for methanol synthesis [170]. Cu_2O with different orientations and thicknesses was deployed in electrocatalysis. The result showed catalyst to be active after reduction to Cu^0 and the selectivity was dependent on the thickness of the oxide [171]. Cyclic voltammetry and electrochemical mass spectrometry evidenced CO_2 reduction only upon Cu_2O reduction to metallic Cu. As observed with in situ Raman spectroscopy, Cu_2O-film reduced to Cu metal at low potentials in aqueous CO_2-saturated 0.1 M $KHCO_3$ [172]. Mandal et al. [173] who combined the DFT study and the in situ Raman with real-time product detection reported a similar observation. It showed that Cu_2O reduction typically precedes CO_2 reduction because the former was energetically more favorable. After reducing Cu_2O to Cu, adsorbed CO, the intermediate in CO_2 reduction, was detected. Copper-complex materials (copper (II) Phthalocyanine, CuPc, HKUST-1 and [Cu(cyclam)]Cl_2)), according to in situ and operando XAS under the working conditions, structurally reconstituted and formed ~2 nm metallic Cu nanoclusters, which catalyzed the conversion of CO_2 to CH_4 during electrocatalytic CO_2 reduction. This was confirmed by DFT calculations which concluded that the restructuring behavior was attributed to the reversible nature of the metal ion–ligand coordination in the structure of copper complex and the generated small size copper clusters under the reaction conditions [174]. An in situ XPS experiment revealed that Cu^0 existed on the surface of CuZnZrGaY catalyst before and after reaction. There was no evidence for the existence of higher oxidation state species as confirmed by the Cu (LMM) Auger spectrum of the catalyst [33]. The CO band frequency attributed to the metallic Cu surface and to oxidized $Cu^{\delta+}$ charged states for some Cu-based catalysts in Table 2 varies due to the presence of different matrices, which act as supports. ZnO as support uniquely influences by shifting the adsorption to lower frequencies, attributed to some sort of interaction with Cu. Moreover, such bands are less intense in comparison with those without the presence of ZnO [175]. The presence of subsurface oxygen was found to modify the electronic structure of Cu and enhance the adsorption of CO, resulting in the existence of Cu in the zero oxidation state according to an investigation using in situ ambient pressure XPS [137]. This means that the presence of sub-surface oxygen influences the activity of Cu.

Table 2. *Measured V_{C-O} associated with metallic Cu on reduced Cu-based catalysts during CO-adsorption at 276 K [175].*

Sample	V_{CO} for metallic Cu surface (cm^{-1})	V_{CO} for $Cu^{\delta+}$ (cm^{-1})
Cu/SiO_2	2100	2125-2127
Raney Cu	2094	2107
Cu/Al_2O_3	2089	2109
Cu/TiO_2	2070	2104-3106
$Cu/ZnO/Al_2O_3$	2065-2068	2093-2100

(ii) Cu-interfacial Sites

The copper-metal/metal oxide (Cu-MO_x) interface has been characterized as active sites for the CO_2 conversion to chemicals [123, 146, 186, 189-193]. Theoretical studies on Cu/ZrO_2 catalysts showed high activity for intermediates formation at the Cu-ZrO_2 interface [123, 189-191]. Liu and co-workers [189, 190] found CO_2 to methanol transformation to be more stable and effective on the Cu/ZrO_2 interface where both the Cu and Zr atoms formed bonds with the reactions species [190]. Polierer et al. [191] found that key intermediates: HCOO, H_2COO, H_2COOH, and H_3CO were linearly correlated with the oxygen's adsorption energy. Behrens et al. [157] found the active sites of a Cu/ZnO catalyst to consist of Cu steps decorated with Zn atoms and stabilized by a series of well-defined bulk defects and surface species. According to the DFT study, Zn-decorated Cu site was more favorable for activating CO_2 to form intermediates and their subsequent hydrogenation to methanol because of its much lower energy barrier of key intermediate step than the pure Cu site [186]. These studies show that Zn and Zr modified the reaction routes in these catalysts compared to the surface of pure Cu. Zn dissolved Cu particles was found as an active sites for methanol production [176, 194]. Laudenschleger et al. [177] recently found the active site on the conventional CO to methanol catalyst ($Cu/ZnO/Al_2O_3$) consisted of non-metallic Zn species with an associated positive charge nature (Cu^0-$Zn^{\delta+}$) under industrial reaction conditions. This active site was investigated by probing the surface of the catalyst with both molecules of "N" reacting species (ammonia, NH_3) and the one that blocks the N species (trimethylamine, TMA), applying an in-house built high-pressure pulse method. The catalyst composition, such as the Cu: ZnO ratio, Cu and ZnO contact, and synthesis route, affected which type of surface sites would be exposed for reaction. These factors could be optimized to maximize the Cu-Zn interface sites [177]. XRD and EDS provided important evidence for the migration of ZnO_x from ZnO to Cu particles to form interfacial Cu-Zn alloy upon reduction with H_2 [167]. The role of ZnO_x is to stabilize the Cu species on the surface, although evidence is only provided for the stabilization as Cu^+ [167, 176, 195, 196]. Such surface species of Cu stabilized by ZnO_x was found to promote methanol synthesis during the hydrogenation of CO_2 [152]. Figure 7 shows the nature of the active sites on the Cu/ZnO catalyst as reported by Tisseraud et al. [152], where the active ZnO_x covers the Cu core. The $Cu/ZnO/Al_2O_3$ catalyst in the reduced state investigated with HRTEM showed an agglomeration of Cu, ZnO, and Al_2O_3 NPs in

proximate contact [163]. The Cu lattice fringes present extended to the surfaces of the NPs without obvious changes in their spacing (d = 2.1 Å) and structure, an observation that indicates the Cu surface in direct contact with the gas environment and covered with a submonolayer of Zn NPs.

Cu-Zn interface was found to be active for both CO_2 adsorption and activation. Also, this surface was actively involved in the production, adsorption and desorption processes of the reactive H_2CO^* species for methanol synthesis [197]. Investigated active sites in other Cu-based catalysts also play relatively similar or slightly different roles. For example, on the La/Cu-SBA-15 catalyst, the Cu-LaO_x interface promoted the adsorption of CO_2 and key intermediates species. The formation of Cu-In alloy on the surface of Cu-In bimetallic catalysts helps to suppress H_2 formation on Cu during CO_2 electrocatalysis.

Bimetallic surfaces have also been identified as the active sites for many Cu-based catalysts, as listed in Table 3. The Cu-Zn bimetallic surface is of several orders of magnitude higher than that of the single Cu surface or the pure ZnO catalysts, resulting from the Cu–Zn synergistic effect [186, 198]. As generally held, Cu is the active site for the Cu/ZnO catalyst, while ZnO modifies Cu and enhances its activity. It has been made evident from recent studies that Zn alloy is hardly stable on Cu (111) and Cu (100) at high temperatures (above 500 K) at which practical CO_2 hydrogenation is carried out. In this case, the Zn–Cu interface formation takes precedence and is beneficial for binding on the catalyst surface and converting CO_2 into intermediate formate species stable on the catalyst surface at high temperatures [196]. Generally, the role of Zn is to improve the performance of Cu catalysts via one or more of the following ways: (a) act as a promoter to promote the structure and modify Cu; (b) enhance the activity, and (c) provide a reservoir for atomic hydrogen storage and use [157, 199]. Metallic Cu NPs on Cu_2O films changed the CO_2 electroreduction product distribution from gaseous to liquid (mainly CH_3OH) on pure Cu_2O. The product change stemmed from the modification of the Cu_2O surface and the formation of Cu/Cu_2O interfaces, which provided sites for binding of H^* and CO^* intermediates in methanol production [187]. The Cu/Cu_2O used as the cathode in the photochemical cell exhibited a good FE for methanol production.

Table 3. *Active sites of Cu-based catalysts in the literature.*

Catalyst	Possible active site structures	Selective species	Ref
Cu/ZnO/Al_2O_3	Zn decorated Cu	MeOH	[157]
CuZnZr	Cu^0	MeOH	[33]
Cu/ZnO, Cu/SiO_2	ZnO_x stabilized Cu^+, Cu-Zn alloy	MeOH	[167, 176]
Cu/ZnO/Al_2O_3, Cu/Zn/Al/Zr	Cu^0 + Cu^+	MeOH	[156, 160]
Cu/ZnO/Al_2O_3	Cu^0-$Zn^{\delta+}$	MeOH	[177]
OD-Cu	Cu^+	C_2H_4	[151]
Cu/ZnO	Cu-Zn alloy	CH_4	[120]
Pd-Cu/SiO_2	Cu-Pd bimetallics	MeOH	[178, 179]
Cu-In-Zr-O	Cu-In_2O_3	MeOH	[162]
Cu/CeO_2/ZrO_2	surface CuO, Cu^{2+}	MeOH	[180]
Cu-In	Cu-In bimetallics	CO	[181]
Cu/ZnO/Al_2O_3	Cu-ZnO interface	MeOH	[164]
Cu/ZnO	ZnO_x	MeOH	[152]
Cu/ZrO_2	Cu-ZrO_2 interface	MeOH	[43, 182, 183]
Cu/ZnO/Al_2O_3	Zn decorated Cu, Cu-Zn alloy	MeOH	[157]
CuO/CeO_2	Cu-CeO_2 interface	MeOH	[166]
Cu/Zr@SiO_2	Isolated Zr (IV)	MeOH	[184]
Cu/Al_2O_3	Cu-Al_2O_3 interface	MeOH, DME, CO	[185]
Cu_2O	Cu_2O (110) (facet)	MeOH	[124].
Cu-Zn	ZnCu (211) (facet)	MeOH	[186]
CuGa alloy	$CuGa_x$, Cu^0, $Ga^{3+}O$	MeOH	[126]
Cu/Cu_2O	Cu/Cu_2O interface	MeOH	[187]
Cu-LaO_x interface	Cu-La/SBA-15	MeOH	[188]

CuO was fully reduced to metallic Cu in the reduced Cu-ZnO catalyst [165]. The Cu crystallite size was used to estimate the metallic Cu surface area, although some researchers apply the chemisorption method using N_2O as a probe molecule to calculate the surface area [200]. The Cu surface area (S_{Cu}) was inversely proportional to the Zn content, but this did not correlate with catalytic activity. It was argued that if the metallic Cu was the active site, TOF versus S_{Cu} should be constant [201]. Opposing, the TOF increased with a decrease in the S_{Cu}, revealing that Cu metal was not the active sites [165, 202]. It has been established that since the metallic Cu surface could not explain the catalyst activity, synergism between the catalyst components (Cu and ZnO) should be relied upon to explain the active site formation. With increasing Zn concentration, the interaction between Cu and ZnO caused the lattice parameter of Cu to expand, indicating an increase in Cu lattice strain and the creation of the Cu–Zn alloy [39, 176]. Kanai et al. [176] observed the formation of Cu–Zn brass-type alloy in Cu-ZnO catalysts reduced at between 250 and 550°C due to the expansion of the lattice Cu when the ZnO content increased. There was a corresponding decrease in the lattices constant of ZnO with decreasing Zn content. The Zn content in the alloy can be determined from the Cu lattice constant. Generally, the content of Zn in Cu-Zn

alloy is high at high reduction temperatures [176].

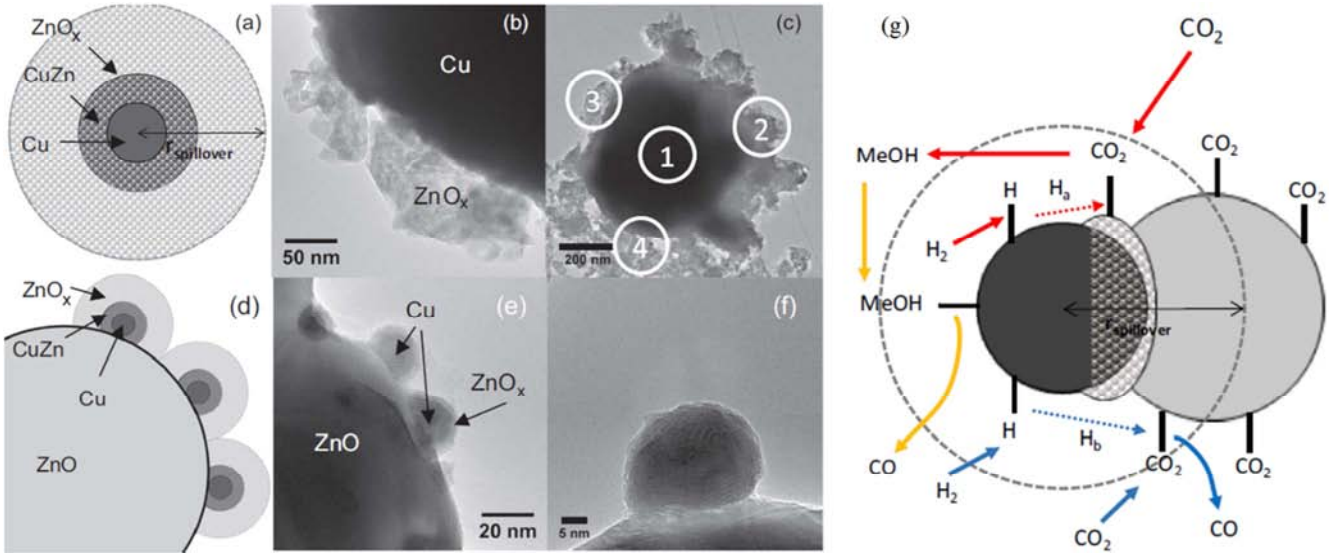

Figure 7. *(a) Model of the methanol synthesis core–shell catalyst, (b and c) TEM image of Cu@ZnO_x catalyst; spots on (c) show presence of Cu and Zn, (d) model of the selective methanol synthesis nano-core–shell catalyst, (e and f) TEM image of Cu@ZnO_x/ZnO catalyst, (g) Model representation of active sites for methanol and CO production from CO_2 hydrogenation over a co-precipitated Cu–ZnO catalyst, pathways to methanol synthesis, RWGS, and methanol decomposition are indicated in red, blue, and yellow arrows, respectively [152].*

(iii) Cu_2O (Cu^+)

Studies have shown that Cu^+ functions in adsorption and stabilization of the intermediates in CO_2 reduction reactions [151, 195, 203, 204]. TPR, and XPS and Raman spectroscopies revealed that Cu exists as Cu^+ species that enable adsorption of CO_2 and serve as active sites for activation of CO_2 molecules on CuO-CeO_2 catalyst in the electroreduction of CO_2 to ethylene [195]. In OD-Cu catalysts for CO_2 electroreduction, Cu^+ sites are good CO-binding sites. On Cu/TiO_2 system, it has been suggested that the active sites for CO_2 photoreduction and methanol production are mainly Cu^+ species [69]. Using in situ XANES, Cu^+ was detected after CO_2 electroreduction to C_{2+} products commenced on OD-Cu catalyst [151, 204]. The residual Cu^+ was crucial to the selectivity of C_2 products. It was found that methanol synthesis on oxidized Cu (100) was higher than that on clean Cu (100) [205], indicating that the Cu ion was the active site. From this study, the mechanism for CO_2 hydrogenation to methanol involves:

a. The adsorption of CO_2 on support.
b. Generation of intermediate species.
c. The dissociative adsorption of H_2 and reaction with intermediate to form methoxy species on the Cu surface.

The CO bond frequency is highly sensitive to the charge on the adsorption site of Cu catalysts [175, 206]. Adsorption of CO was observed on reduced Cu/ZnO/SiO_2 and Cu/SiO_2 catalysts [206]. In both catalysts, Cu^+ species were not stabilized by the ZnO component. A high CO adsorption was recorded on Cu^+ sites while the adsorption on Cu^0 sites was moderate. The Cu/ZnO/Al_2O_3 catalyst showed CO adsorption band at frequencies (2065–2094 cm^{-1}) [38, 175, 207, 208]. Upon surface coverage with adsorbate such as formed formate during CO_2 reduction to methanol, electron transfer (withdrawing effect of formate) takes effect, leading to an upward shift in the CO stretching frequency. The molecular CO can form carbonyls (Cu^+–CO) with IR bands in the range 2160–2080 cm^{-1} upon strong adsorption onto Cu^+ sites [167, 209]. The formation of stable carbonyls with Cu^{2+} ions at ambient temperature has not been reported [210]. In a study by Kanai et al. [167], the CO adsorption sites were assigned to Cu^+–O–Zn species. When the Cu/ZnO catalysts were exposed to the reactant gas atmosphere (CO_2–H_2), Zn oxidized by CO_2 to Cu^+–O–Zn, which usually contained ZnO_x moieties that have been identified as active sites for methanol synthesis [152].

A Cu/Pt-TiO_2 co-catalysts prepared by the stepwise photodeposition technique of Pt NPs and then Cu onto TiO_2 revealed the formation of a core-shell catalyst with Cu covering the Pt core according to the HRTEM imaging. Both the irradiation time and the Cu content were found to affect the catalyst structure. The lattice fringes with an interplanar spacing of 0.211 nm revealed by the HRTEM analysis suggested the formation of Cu_2O on the shell, that is, Cu existed in the Cu^+ state [203]. Further characterization using XRD revealed diffraction peaks belonging to the TiO_2. The XPS binding energy of Cu $2p_{3/2}$ for the catalysts at about 932.5 eV suggested the presence of Cu^0 and Cu^+. With the Cu (LLL) Auger spectrum, only Cu^+ was observed, which corresponded to the HRTEM result. However, it should be noted that Cu^0 is easily oxidized to Cu^+ under experimental conditions or on exposure to air [211, 212].

The in situ synchrotron powder diffraction (SPD) experiments were conducted to determine the active sites and understand their dynamic changes during electrocatalytic reduction of CO_2 over Cu/graphene and Cu/graphene-Ar [121]. During a 90 min CO_2 reduction, the results showed

characteristic peaks of Cu_2O (002), Cu_2O (222), Cu (111), Cu (002) and Cu (002) in the diffraction patterns of Cu/graphene and Cu/graphene-Ar. It was observed that graphene-supported Cu showed a feature of CuO phase that directly transformed to the Cu (111) phase. Both Cu_2O and Cu phases stabilized on the Cu/graphene-Ar. This study identifies Cu_2O as the active Cu species in electrochemical CO_2 reduction to hydrocarbons because CuO exhibited poor adsorption for CO_2 molecules, and hence, less active for CO_2 reduction. Also, CuO phase was directly reduced to metallic Cu rather than Cu_2O. Hence, the superior CO_2 reduction performance of Cu/graphene-Ar was attributed to its ability to form a higher content of surface Cu_2O species during its synthesis and maintain it under relevant reaction conditions and the easy transformation of CuO to metallic Cu [121].

(iv) Mixed/Other Cu Species

The mixture of Cu^+ and Cu^0 can be beneficial for the adsorption and splitting of H_2. XPS measurements revealed Cu/TiO_2 and $Cu/Pt\text{-}TiO_2$ catalysts contained Cu either in the chemical state of 0 or +1 [211]. Previous data showed that catalytic products might change as a result of catalytic surfaces with varying compositions of Cu^0 and Cu^+; surface with higher content of Cu^0 led to CO, while that with mixed Cu^0 and Cu^+ resulted in C_2 products such as ethanol [95]. The mixed oxidation states of Cu can improve reactivity and selectivity toward C_{2+} products by way of enhancing CO_2 adsorption on one site and C-C coupling on another site [213]. For example, the C-C coupling reaction of two $^*CHO$ species can occur on the Cu^0–$Cu^{\delta+}$ atomic interface with a low kinetic barrier of 0.57 eV in the formation of ethanol [213]. According to Tseng et al. [214], a relationship exists between the chemical states of Cu and methanol production on Cu/TiO_2 catalysts which increased in the order of $Cu^{2+} > Cu^+ > Cu^0$ through formate and methoxy-intermediates on the Cu sites, facilitating the electron transfer from the catalyst surface [215, 216]. Compared with bulk crystalline Cu_2O with Cu–O bond lengths of 1.86 Å, the Cu–O bond lengths of 1.92–1.95 Å was calculated around the CO_2 and H_2O adsorption sites, characteristic of the DFT calculated Cu–O of 1.95 Å in bulk crystalline CuO [124]. XANES and EXAFS are reliable techniques for characterizing the electronic states and local structure of Cu and ZnO in Cu/ZnO-based catalysts (e.g., CuO/ZnO, $CuO/ZnO/Al_2O_3$, and $CuO/ZnO/Al_2O_3/ZrO_2$) by measuring the Cu K-edge and Zn K-edge regions [217-219]. The Cu K-edge XANES spectra of $CuO/ZnO/Al_2O_3/ZrO_2$ mixed oxide catalysts exhibited XANES spectra similar to that of CuO at 8984 eV, suggesting the presence of Cu^{2+} species [217]. Under working conditions, the nature of the active catalyst remained unchanged despite an obvious change in methanol yield. This observation needs further investigations to rule out the possibility of missing data. The suboxidic species have also been detected experimentally [95, 220-222] and EXAFS characterization confirmed an average Cu-O coordination number of 1.1 for suboxidic Cu [222]. Because of reaction intermediates and surface polarization generated by the applied electric potential, most Cu-based catalysts reconstruct under reaction conditions [223, 224]. Species specified by their coordination and charges occur upon reconstruction, regardless of the starting structure: Cu^0 and oxidized Cu ($Cu^{\delta+}$ and Cu^+) [103, 213, 220]. The $Cu^{\delta+}$ on Cu^0 surface is critical to the activity and selectivity of electrochemical reduction of CO_2 [220].

During CO electroreduction on OD-Cu catalysts, high CO reduction activity was linked with surface sites that bound CO more strongly than low-index and stepped Cu facets, attributed to the metastable sites from the disordered surfaces at the grain boundary and defect terminations stabilized by the interconnected nanocrystalline network [141]. By reducing mixtures of ^{13}CO and $^{12}CO_2$, Lum et al. [225] showed that OD-Cu catalysts possess product-specific sites for C–C coupled products. Three different types of active sites were identified, each for a different product. In a follow-up study combining theoretical and experimental techniques, planar-square and convex-square sites were identified as the active sites for ethylene production, while step-square sites were responsible for generating C_{2+} alcohols [226].

3.2.3. Catalyst Structural Characterization by Advanced and Integrated in Situ Techniques

(i) A Simple Comparison of Various Characterization Techniques

One of the major challenges impeding the rational design of heterogeneous catalysts for CO_2 transformation is the structural complexity, impairing our comprehension of the reaction mechanism and catalyst design efforts [158, 197]. Researchers commonly deploy various characterization techniques to determine the structure-activity relationships of the Cu-based catalysts, including theoretical, microscopic (imaging), spectroscopic, and chemisorption methods [33, 124, 158, 188-190, 209, 217, 227]. These tools can offer key information of the catalyst structure, such as the active sites and the intermediates species of CO_2 reduction reactions. Recently, the accuracy of the information on the catalyst structure has improved with the development and deployment of advanced characterization and theoretical methods. The emergence of in situ/operando characterization techniques is one of the exciting developments in catalysis research in the last several decades that have revolutionized catalysis and facilitated measurements under controlled environments and practical catalyst working conditions. These techniques include X-ray diffraction/scattering (XRD), X-ray photoelectron spectroscopy (XPS), X-ray absorption spectroscopy (XAS), transmission electron microscopy (TEM), and other methods developed and deployed in unraveling the structure-activity relationships, reaction mechanisms and for understanding the reaction evolutional and dynamic changes in real-time [227-230]. With these developments, it is becoming easier to investigate the catalytic surfaces under reaction conditions. For example, in situ STM can image ceria islands of about one layer thick, exhibiting rough surfaces with a CeO_2 (111) termination in the $CeO_2/Cu_2O/Cu$ catalyst for methanol production from CO_2 in real-time process [166]. In situ surface-enhanced infrared

absorption spectroscopic (SEIRAS) can selectively probe species adsorbed on the metal surface to a depth of <10 nm [140].

It takes a very short time (a few minutes) for the metal oxidation state to reach a steady-state under the CO_2 reduction condition; thus, a time-resolved determination of the oxidation state of metal centers, especially at a time-scale of a few seconds, should be pursued [95]. For example, CuO_x precursor would attain a steady-state condition in a few seconds according to the data from in situ Raman spectroscopy in electrocatalysis due to the simultaneous occurrence of electrochemical reduction and spontaneous oxidation [231]. Therefore, analysis of such catalysts under real-time is recommended. The application of some in situ techniques is limited due to special operation requirements. For example, in situ ambient pressure X-ray photoelectron spectroscopy (APXPS) requires ultra-high vacuum (UHV) condition to function properly. However, using the synchrotron radiation for APXPS can overcome this limitation [229]. The invention and application of APXPS represent a key advancement in the in situ XPS technique. Other techniques have witnessed advances too, such as the TEM in which the development of environmental TEM (ETEM) has enabled the in situ characterization of structural evolution of single-atom catalyst [227]. It is now possible to obtained sub-Angstrom's resolution imaging and analysis by using image or probe aberration-corrected TEM instruments. In situ TEM can reveal growth transformation and function in nanomaterials [232]. Further advances should rely on developing new in situ techniques combining multiple complementary characterization techniques that simultaneously compare results.

Table 4. *Common techniques for characterizing Cu-based catalyst properties.*

Techniques	Principle	Specific application	Merit	Demerit
Scanning Tunneling Microscopy (STM)	Based on quantum tunneling	-Arrangement of atoms on metal Cu surfaces -Elucidates promoters role -Examines adsorption or diffusion of intermediate species	-Provides surface information -Operates at ambient conditions	-Complexity of result interpretation, -Requires neat and clean surface
Transmission Electron microscopy (TEM)	Based on electron transmission	-Cu atomic structures -Shape of Cu metal particles	-Can penetrate a few layers deep	-Sample preparation needs carefulness, -High operation voltage
X-ray photoelectron spectroscopy (XPS)	Based on external photoelectric effect	-Oxidation states of Cu	-Surface elemental composition -Identifies oxidation state -High sensitivity	-Cannot distinguish oxidation states of negligible energy difference -Requires complementary technique such as Auger electron spectroscopy
X-ray absorption spectroscopy (XAS) – EXAFS and XANES	Excitation of core-level electrons to vacant valence states	-Determines electronic structure - Determines geometry - Determines coordination environment and Symmetry	-Examines structure of specific elements -Determines oxidation state	-Short-range order -Bulk information -Limited sensitivity
X-ray diffraction (XRD)	Diffuse and/or coherent scattering of incident X-rays	-Elucidation of Cu phases -Structure and crystallinity of Cu crystal -Lattice parameters of metallic Cu	-Provides information about the NP's size -Interatomic distance of X-ray scattering atomic pairs	-Gives bulk information -Low sensitivity to amorphous materials
Infrared (IR) spectroscopy	Interaction of infrared radiation with sample	-CO adsorbed IR spectroscopy can distinguish the oxidation states of Cu (Table 5) -Intermediate species	-Identifies functional groups, chemical species, -Easy determination of intermediate species	-Band assignment of impure catalytic material is difficult
Electron Paramagnetic Resonance (EPR)	Based on paramagnetism due unpaired electron spins	-Determines isolated Cu^{2+} sites	-Highly sensitive -Provides quantitative data -Provides information about ZnO -Detects electron binding and transfer	-Requires presence of unpaired electrons -Needs transition between spin states -Low temperature requirement -Cannot detect Cu^0 and Cu^+
Density Functional Theory (DFT)	Operates based on functional of electron density	-Gives binding and adsorption energy of Cu sites Can compute -Cu-Cu, Cu-O, C-O and C-C bond lengths	Reduced computational cost -Calculation of large systems (e.g., metal NPs and periodic surfaces)	-Complicated calculations -Time consuming

Computational methods have also been utilized for analyzing the catalyst structure, including DFT, kinetic Monte Carlo simulation, and microkinetics modeling [145, 186, 191]. DFT, the most widely used approach, uses electron density functions to determine ground-state energy and properties derived from it. It has the advantage of low computational cost and being able to calculate larger systems like metal NPs and periodic surfaces. Moreover, results from theoretical studies are used as a validation of the experiments, thus can compensate for experimental deficits. DFT calculations have been applied to elucidate the roles of Cu and ZnO species at the Cu–ZnO interfacial sites, and the participation of the Cu–Zn sites over metallic Cu (211) surface and Cu–Zn alloy in methanol synthesis [157, 186]. Combining the theoretical studies in real-time with state-of-the-art in situ characterization techniques is an innovation the field of

research is urgently needing. To help understand the different functions of various characterization techniques as applied to Cu-based catalysts for CO_2 reduction, we summarize and compare these techniques in Table 4.

Table 5. *CO stretching frequencies (ν_{CO}) for CO adsorbed on Cu surfaces or on isolated Cu ions. Data extracted from ref. [175]*

Cu species	CO stretching frequencies (cm^{-1})
Isolated Cu^+ ion	2215
Cu^{2+} surface sites	2240–2150
Cu^+ surface sites	2160–2100
Stepped Cu metal surface	2110–2100
Planar Cu metal surface	2100–2070
Negatively charged Cu metal	2070–2038
Isolated Cu^- ion	1743

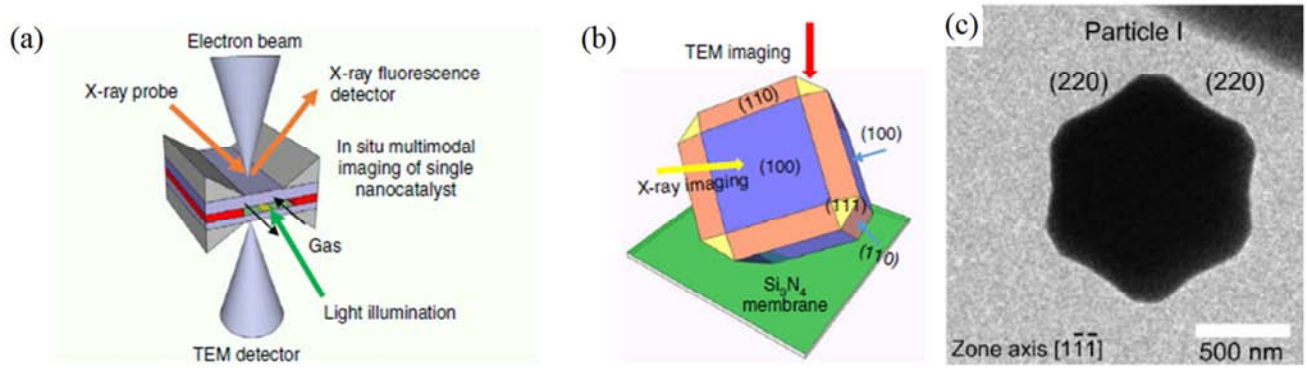

Figure 8. *Operando characterization of a single Cu_2O particle photocatalyst (a) Setup showing the gas-flow nanoreactor, (b) Schematic of the electron beam and X-ray directions for TEM and SFXM imaging on a catalyst particle, (c) TEM of a catalyst particle [124].*

(ii) Catalyst Structural Characterization by Integrated Methods

The characterization of single particles of a catalyst is possible with the use of advanced characterization techniques such as environmental transmission electron microscopy (ETEM) [233] and scanning fluorescence X-ray microscopy (SFXM) [124]. Photocatalytic Cu particles have been investigated with these techniques during the photoreduction of CO_2 [124, 234]. Wu et al. [124] studied the local crystal structure of a single Cu_2O particle used as catalyst for the photochemical reduction of CO_2 under typical working conditions. The catalyst was exposed to a gaseous mixture of CO_2 and steam, and irradiation source as arranged in Figure 8. The edges of the catalyst particle were found to correspond to the (220) planes by single-particle electron diffraction (SPED) (Figure 8c). The spatial location of the particle was determined using low-resolution scans employing Cu fluorescence signals from Cu_2O particles. A specific facet of the particle can be focused by the X-ray beam parallel to desired facets while scanning of the incident X-ray energy, allowing facet-dependent spectroscopic information on the Cu active sites to be obtained. A white-line peak at 8981.0 eV was found in the X-ray fluorescence spectra recorded at the Cu K edge on the (110) facet of a Cu_2O particle, indicating a Cu^+ oxidation state associated with this facet. The spectral peak observed on the (100) facet at 8981.5 eV indicates the existence of both Cu^+ and Cu^{2+} charged states. Furthermore, information on the change in the oxidation state can equally be obtained. For example, the peak shift of between 1.0 and 1.5 eV towards higher energy from low energy is an indication of the change from +1 to +2 oxidation state of Cu or vice versa depending on the exposed conditions. With the aid of this technique, it was revealed that the (110) facet Cu_2O photocatalyst particle was the active sites for CO_2 reduction to methanol during photocatalysis while Cu_2O (100) facet was photocatalytically non-reactive. The ETEM images of Cu NPs on ZnO under different gas mixtures revealed the Cu NPs to be flat-like and spherical under reducing and oxidizing conditions, respectively [233]. That is, the particles changed shape (reconstructed) with changes in gas composition. High-resolution X-ray powder diffraction (HRXRD) and EPR were further applied to characterize the photocatalytically active sites of the Cu_2O particles ensembles. The results revealed the obvious structural changes over the course of the reaction, which was monitored with the operando high-energy XRD. Data from this measurement showed that in the absence of light, the co-adsorption of $CO_2/H_2O_{(g)}$ increased the crystal lattice constant, confirming the electron density withdrawal effect of CO_2 on Cu active sites which caused an oxidation state transition from Cu^+ to Cu^{2+} [124]. Photocatalytic reduction of CO_2 to liquid fuels by a photoinduction method was utilized to form Cu single atoms on the UiO-66-NH_2 support (Cu SAs/UiO-66-NH_2) [235]. The catalyst local structure was measured with XAFS which found the absorption edge positions located between that of Cu and CuO, suggesting a positively charged Cu state between 0 and +2 [235]. It was found that isolated Cu atoms were fixed at the atomic level in the UiO-66-NH_2 matrix and were coordinated to two N atoms with atoms distance of 1.97 Å (Cu−N). Confirming using the Fourier-transformed (FT) EXAFS, one main peak at 1.50 Å in the FT-EXAFS spectrum was observed, corresponding to the first coordination shell of Cu−N. A

similar result was observed with the wavelet transformation (WT) plot of Cu SAs/UiO-66-NH_2, which showed the WT maximum at 3.8 $Å^{-1}$, ascribed to Cu−N bonding. The peak at 2.3 Å, corresponding to Cu−Cu, was lacking in the case of Cu SAs/UiO-66-NH_2. From both measurements, there was no observation attributed to Cu−Cu for Cu SAs/UiO-66-NH_2. The catalyst achieved a photocatalytic conversion of CO_2 to CH_3OH and C_2H_5OH with an evolution rate of 5.33 and 4.22 μmol $h^{-1}g^{-1}$, respectively.

Mistry et al. [151] investigated the surface species and structural changes in the oxide layer during CO_2 electroreduction by applying operando XANES and EXAFS. The results in Figure 9 revealed the prominent shoulder at ~8,982 eV on the XANES spectrum of the plasma-oxidized Cu, a feature of Cu_2O. The existence of metallic Cu and Cu oxides in the catalyst can be clearly observed in the EXAFS spectrum (Figure 9 b and c). Upon the partial reduction of the film, XAFS spectra showed a dominantly metallic Cu underlayer signal. This technique can show without doubt the presence of the different Cu species viz- Cu_2O, CuO, and metallic Cu, although the oxidic species were evident only for the oxidized catalysts. While reduction of the oxide phases was also visualized, reconstruction was such that the Cu_2O remained highly stable, and thus it was concluded that Cu^+, which was supplied from oxide surface and subsurface layers during the reaction, was the active reaction phase.

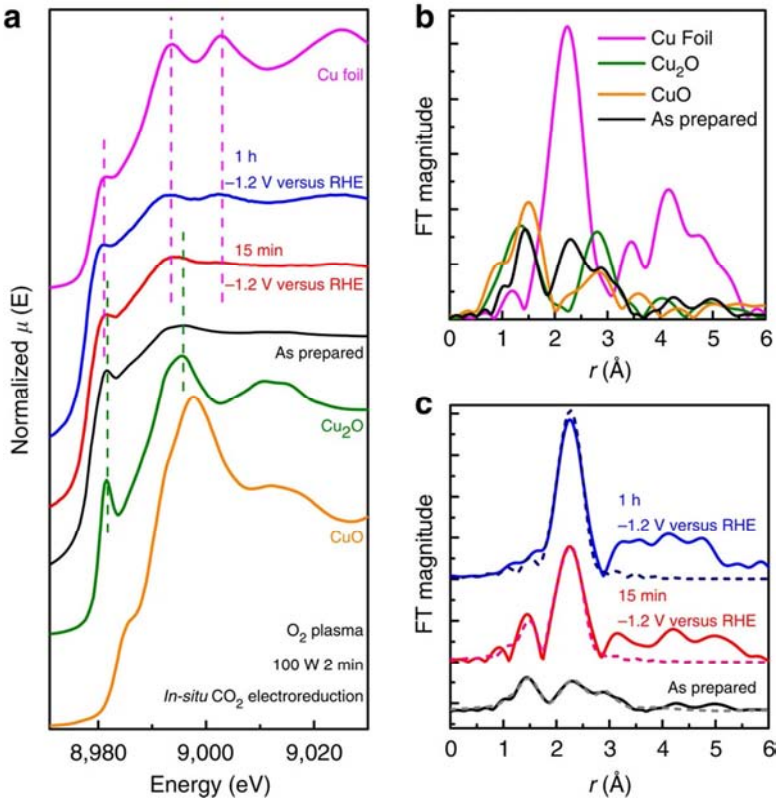

Figure 9. *Operando structural characterization of plasma activated Cu-based catalyst in CO_2 electroreduction measured under operando conditions (a) XANES spectra of the O_2 treated for 2 min at 100 W, (b) EXAFS spectra of prepared and reference samples, (c) EXAFS spectra and fits of prepared sample [151].*

4. Conclusion and Future Perspective

This report reviews the Cu-based catalysts for the CO_2 valorization, the key information about the nature and possible structures of the active sites in them. Also, it compares the techniques developed for their characterizations. The obtained information about the catalyst active sites can guide the catalyst development and help understand the real catalysis on the catalyst surface.

Capturing and transforming CO_2 into useful products is an efficient and economical way to reduce carbon footprint and achieve near-neutral CO_2 emission. Promoted and/or supported Cu catalysts is efficient for thermochemical CO_2 conversion to products like methanol and methane. On the other hand, these catalysts are less efficient when light or electricity are applied for CO_2 conversion. CuO_x oxides are more active catalysts for the photochemical process. Cu supported on CuO_x or its inverse referred to as oxide-derived catalyst (OD-Cu) shows superior activity for conversion CO_2 in the electrochemical process. The performances of the different kinds of Cu catalysts depend on the quality and quantity of the active site in them.

Active sites play essential roles in accurately determining the reaction mechanisms and general properties of heterogeneous catalytic reactions. The activity, selectivity, and stability of a catalyst are all influenced by the kind and nature of active sites. For CO_2 conversion, the Cu active sites include but are not limited to metallic Cu, Cu_2O, and Cu-metal/Cu-metal oxide interfaces. Underexplored structures of the Cu surface, such as suboxidic Cu surface, can drive CO_2 reduction. The mixed active sites can even

drive further the selectivity toward different products. Therefore, engineering of such active sites on the same surface apparently can improve the selectivity of a specific product.

The dynamic behaviors during catalytic processes make the identification and investigation of the active sites still challenging, often because of the reconstruction of the surface by reaction intermediates and polarization caused by reaction conditions. However, significant progress has been achieved in the last two decades, thanks to state-of-the-art characterization techniques and advanced computation methods. These include the following strategies developed and deployed. (1) Development of individual in situ and operando techniques that are highly sensitive, accurate, and precise for characterizing the structure and active sites under ideal working conditions can further reveal the real active sites of Cu catalyst systems. For example, X-ray microscopy can map the active states of nanocatalysts under typical relevant reaction conditions. (2) Several advanced techniques, e.g., real-time product detection, theoretical calculations, and operando surface spectroscopy, can be simultaneously deployed. Raman spectroscopy, for instance, can be combined with selected-ion flow tube mass spectrometry (SIFT-MS); this strategy can in real-time examine the catalyst surface and detect the multicomponent products generated in situ during a reaction. Furthermore, SIFT-MS can simultaneously quantify multi-component products with finite vapor pressure in a split of seconds (typically 0.1 to 10 sec). This technique allows to capture reaction dynamics early enough and eliminate issues associated with the analysis of gaseous products of CO_2 reaction with conventional gas chromatography that needs longer analysis time and waiting till the end of the reaction. Furthermore, with these measurements, the dynamic structures of the active sites can be understood further, which can be used to guide the rational design of novel catalysts and modify the existing ones for optimum performance.

Developing novel high-performing catalysts for CO_2 conversion is needed as part of controlling CO_2 emission efforts. Although many catalysts have been developed, they are not good enough for the targeted catalytic conversion reactions. Tailoring active sites on a catalyst could drive the selectivity to a given product. Maximizing the sites selective to the target product and minimizing those to the undesirable product can be an important strategy to achieve this aim. For example, the design of Cu particles covered with ZnO_x of thickness greater than the diffusion sphere of H_2 to inhibit the RWGS reaction is suggested. Core-shell systems are well-suited structures that can fulfill these specifications, such as a $Cu@MO_x$ catalyst. Additionally, the size of the core-shell particles must be controlled to reach a high dispersion and high surface area of the exposed ZnO_x active phase. This division could introduce function-specific roles such that only reaction for the formation of desirable product is promoted over undesirable product formation. It remains to be shown whether practical strategies exist for further increasing the step/defect density in Cu NPs. In general, the future Cu catalysts for CO_2 conversion should be well-engineered at the surface towards a specific reaction product to eliminate the need to control the reaction conditions to improve catalyst activity.

Acknowledgements

This work is financially supported by the 2020 Li Ka Shing Foundation Cross-Disciplinary Research Grant (2020LKSFG09A), by the Guangdong Province Key discipline fund (GTIIT) in 2021, and by the GTIIT Project KD2000079.

References

[1] Obama, B. (2017). The irreversible momentum of clean energy. Science, 355, 126.

[2] Durrani, J., Can catalysis save us from our CO_2 problem?, Chemistry World, 2019.

[3] Wang, J., Huang, L., Yang, R., Zhang, Z., Wu, J., Gao, Y., Wang, Q., O'Hare, D., Zhong, Z. (2014). Recent advances in solid sorbents for CO_2 capture and new development trends. Energy Environ Sci, 7, 3478-3518.

[4] Wang, Q., Luo, J., Zhong, Z., Borgna, A. (2011). CO_2 capture by solid adsorbents and their applications: current status and new trends. Energy Environ Sci, 4, 42-55.

[5] Kumaravel, V., Bartlett, J., Pillai, S. C. (2020). Photoelectrochemical conversion of carbon dioxide (CO_2) into fuels and value-added products. ACS Energy Letters, 5, 486-519.

[6] Ra, E. C., Kim, K. Y., Kim, E. H., Lee, H., An, K., Lee, J. S. (2020). Recycling carbon dioxide through catalytic hydrogenation: recent key developments and perspectives. ACS Catal, 10, 11318-11345.

[7] Jones, W. D. (2020). Carbon Capture and Conversion. J Am Chem Soc, 142, 4955-4957.

[8] Das, S., Pérez-Ramírez, J., Gong, J., Dewangan, N., Hidajat, K., Gates, B. C., Kawi, S. (2020). Core–shell structured catalysts for thermocatalytic, photocatalytic, and electrocatalytic conversion of CO_2. Chem Soc Rev, 49, 2937-3004.

[9] Artz, J., Müller, T. E., Thenert, K., Kleinekorte, J., Meys, R., Sternberg, A., Bardow, A., Leitner, W. (2018). Sustainable conversion of carbon dioxide: an integrated review of catalysis and life cycle assessment. Chem Rev, 118, 434-504.

[10] Etim, U., Song, Y., Zhong, Z. (2020). Improving the Cu/ZnO-Based Catalysts for Carbon Dioxide Hydrogenation to Methanol, and the Use of Methanol As a Renewable Energy Storage Media. Frontiers in Energy Research, 8.

[11] Deng, Y., Yeo, B. S. (2017). Characterization of Electrocatalytic Water Splitting and CO_2 Reduction Reactions Using In Situ/Operando Raman Spectroscopy. ACS Catal, 7, 7873-7889.

[12] Rahbari, A., Ramdin, M., Van Den Broeke, L. J., Vlugt, T. J. (2018). Combined steam reforming of methane and formic acid to produce syngas with an adjustable H_2: CO ratio. Ind Eng Chem Res, 57, 10663-10674.

[13] Ye, R.-P., Ding, J., Gong, W., Argyle, M. D., Zhong, Q., Wang, Y., Russell, C. K., Xu, Z., Russell, A. G., Li, Q. (2019). CO_2 hydrogenation to high-value products via heterogeneous catalysis. Nat Commun, 10, 1-15.

[14] Zhang, X., Zhang, G., Song, C., Guo, X. (2020). Catalytic Conversion of Carbon Dioxide to Methanol: Current Status and Future Perspective. Frontiers in Energy Research, 8, 413.

[15] Li, Z., Das, S., Hongmanorom, P., Dewangan, N., Wai, M. H., Kawi, S. (2018). Silica-based micro-and mesoporous catalysts for dry reforming of methane. Catal Sci Technol, 8, 2763-2778.

[16] Currie, R., Mottaghi-Tabar, S., Zhuang, Y., Simakov, D. S. (2019). Design of an Air-Cooled Sabatier Reactor for Thermocatalytic Hydrogenation of CO_2: Experimental Proof-of-Concept and Model-Based Feasibility Analysis. Ind Eng Chem Res, 58, 12964-12980.

[17] Atsonios, K., Panopoulos, K. D., Kakaras, E. (2016). Thermocatalytic CO_2 hydrogenation for methanol and ethanol production: Process improvements. Int J Hydrog Energy, 41, 792-806.

[18] De, S., Dokania, A., Ramirez, A., Gascon, J. (2020). Advances in the Design of Heterogeneous Catalysts and Thermocatalytic Processes for CO_2 Utilization. ACS Catal, 10, 14147-14185.

[19] Simakov, D. S. A. Electrocatalytic Reduction of CO_2, In: Renewable Synthetic Fuels and Chemicals from Carbon Dioxide: Fundamentals, Catalysis, Design Considerations and Technological Challenges, Springer International Publishing, Cham, 2017, pp. 27-42.

[20] Simakov, D. S. A. Thermocatalytic Conversion of CO_2, Renewable Synthetic Fuels and Chemicals from Carbon Dioxide: Fundamentals, Catalysis, Design Considerations and Technological Challenges, Springer International Publishing, Cham, 2017, pp. 1-25.

[21] Simakov, D. S. A. Photocatalytic Reduction of CO_2, Renewable Synthetic Fuels and Chemicals from Carbon Dioxide: Fundamentals, Catalysis, Design Considerations and Technological Challenges, Springer International Publishing, Cham, 2017, pp. 43-54.

[22] Kho, E. T., Tan, T. H., Lovell, E., Wong, R. J., Scott, J., Amal, R. (2017). A review on photo-thermal catalytic conversion of carbon dioxide. Green Energy & Environment, 2, 204-217.

[23] Zhang, N., Long, R., Gao, C., Xiong, Y. (2018). Recent progress on advanced design for photoelectrochemical reduction of CO_2 to fuels. Science China Materials, 61, 771-805.

[24] Chan, K., Tsai, C., Hansen, H. A., Nørskov, J. K. (2014). Molybdenum sulfides and selenides as possible electrocatalysts for CO_2 reduction. ChemCatChem, 6, 1899-1905.

[25] Xie, B., Wong, R. J., Tan, T. H., Higham, M., Gibson, E. K., Decarolis, D., Callison, J., Aguey-Zinsou, K.-F., Bowker, M., Catlow, C. R. A. (2020). Synergistic ultraviolet and visible light photo-activation enables intensified low-temperature methanol synthesis over copper/zinc oxide/alumina. Nat Commun, 11, 1-11.

[26] Jiang, X., Nie, X., Guo, X., Song, C., Chen, J. G. (2020). Recent Advances in Carbon Dioxide Hydrogenation to Methanol via Heterogeneous Catalysis. Chem Rev.

[27] Kattel, S., Liu, P., Chen, J. G. (2017). Tuning selectivity of CO_2 hydrogenation reactions at the metal/oxide interface. J Am Chem Soc, 139, 9739-9754.

[28] Dang, S., Yang, H., Gao, P., Wang, H., Li, X., Wei, W., Sun, Y. (2019). A review of research progress on heterogeneous catalysts for methanol synthesis from carbon dioxide hydrogenation. Catal Today, 330, 61-75.

[29] Goeppert, A., Czaun, M., Jones, J.-P., Prakash, G. S., Olah, G. A. (2014). Recycling of carbon dioxide to methanol and derived products–closing the loop. Chem Soc Rev, 43, 7995-8048.

[30] Paulino, P., Salim, V., Resende, N. (2016). Zn-Cu promoted TiO_2 photocatalyst for CO_2 reduction with H_2O under UV light. Appl Catal B: Environ, 185, 362-370.

[31] French, S., Sokol, A., Bromley, S., Catlow, C., Sherwood, P. (2003). Identification and characterization of active sites and their catalytic processes—the Cu/ZnO methanol catalyst. Top Catal, 24, 161-172.

[32] Yang, H., Zhang, C., Gao, P., Wang, H., Li, X., Zhong, L., Wei, W., Sun, Y. (2017). A review of the catalytic hydrogenation of carbon dioxide into value-added hydrocarbons. Catal Sci Technol, 7, 4580-4598.

[33] Natesakhawat, S., Lekse, J. W., Baltrus, J. P., Ohodnicki Jr, P. R., Howard, B. H., Deng, X., Matranga, C. (2012). Active sites and structure–activity relationships of copper-based catalysts for carbon dioxide hydrogenation to methanol. ACS Catal, 2, 1667-1676.

[34] Toyir, J., de la Piscina, P. R. r., Fierro, J. L. G., Homs, N. s. (2001). Catalytic performance for CO_2 conversion to methanol of gallium-promoted copper-based catalysts: influence of metallic precursors. Appl Catal B: Environ, 34, 255-266.

[35] Toyir, J., de la Piscina, P. R. r., Fierro, J. L. G., Homs, N. s. (2001). Highly effective conversion of CO_2 to methanol over supported and promoted copper-based catalysts: influence of support and promoter. Appl Catal B: Environ, 29, 207-215.

[36] Suh, Y.-W., Moon, S.-H., Rhee, H.-K. (2000). Active sites in $Cu/ZnO/ZrO_2$ catalysts for methanol synthesis from CO/H_2. Catal Today, 63, 447-452.

[37] Dong, X., Li, F., Zhao, N., Xiao, F., Wang, J., Tan, Y. (2016). CO_2 hydrogenation to methanol over $Cu/ZnO/ZrO_2$ catalysts prepared by precipitation-reduction method. Appl Catal B: Environ, 191, 8-17.

[38] D'Alnoncourt, R. N., Xia, X., Strunk, J., Löffler, E., Hinrichsen, O., Muhler, M. (2006). The influence of strongly reducing conditions on strong metal–support interactions in Cu/ZnO catalysts used for methanol synthesis. Phys Chem Chem Phys, 8, 1525-1538.

[39] Günter, M. M., Ressler, T., Bems, B., Büscher, C., Genger, T., Hinrichsen, O., Muhler, M., Schlögl, R. (2001). Implication of the microstructure of binary Cu/ZnO catalysts for their catalytic activity in methanol synthesis. Catal Lett, 71, 37-44.

[40] Grunwaldt, J.-D., Molenbroek, A., Topsøe, N.-Y., Topsøe, H., Clausen, B. (2000). In situ investigations of structural changes in Cu/ZnO catalysts. J Catal, 194, 452-460.

[41] Li, W., Lu, P., Xu, D., Tao, K. (2018). CO_2 hydrogenation to methanol over Cu/ZnO catalysts synthesized via a facile solid-phase grinding process using oxalic acid. Korean J Chem Eng, 35, 110-117.

[42] Ojelade, O. A., Zaman, S. F. (2019). A Review on Pd Based Catalysts for CO_2 Hydrogenation to Methanol: In-Depth Activity and DRIFTS Mechanistic Study. Catal Surv Asia, 1-27.

[43] Kattel, S., Yan, B., Yang, Y., Chen, J. G., Liu, P. (2016). Optimizing binding energies of key intermediates for CO_2 hydrogenation to methanol over oxide-supported copper. J Am Chem Soc, 138, 12440-12450.

[44] Huš, M., Dasireddy, V. D., Štefančič, N. S., Likozar, B. (2017). Mechanism, kinetics and thermodynamics of carbon dioxide hydrogenation to methanol on $Cu/ZnAl_2O_4$ spinel-type heterogeneous catalysts. Appl Catal B: Environ, 207, 267-278.

[45] Huš, M., Kopač, D., Štefančič, N. S., Jurković, D. L., Dasireddy, V. D., Likozar, B. (2017). Unravelling the mechanisms of CO_2 hydrogenation to methanol on Cu-based catalysts using first-principles multiscale modelling and experiments. Catal Sci Technol, 7, 5900-5913.

[46] Karelovic, A., Galdames, G., Medina, J. C., Yévenes, C., Barra, Y., Jiménez, R. (2019). Mechanism and structure sensitivity of methanol synthesis from CO_2 over SiO_2-supported Cu nanoparticles. J Catal, 369, 415-426.

[47] Yang, B., Liu, C., Halder, A., Tyo, E. C., Martinson, A. B., Seifert, S. n., Zapol, P., Curtiss, L. A., Vajda, S. (2017). Copper cluster size effect in methanol synthesis from CO_2. J Phy Chem C, 121, 10406-10412.

[48] Liu, C., Liu, P. (2015). Mechanistic study of methanol synthesis from CO_2 and H_2 on a modified model Mo_6S_8 cluster. ACS Catal, 5, 1004-1012.

[49] Grabow, L., Mavrikakis, M. (2011). Mechanism of methanol synthesis on Cu through CO_2 and CO hydrogenation. ACS Catal, 1, 365-384.

[50] Inoue, T., Fujishima, A., Konishi, S., Honda, K. (1979). Photoelectrocatalytic reduction of carbon dioxide in aqueous suspensions of semiconductor powders. Nature, 277, 637-638.

[51] Indrakanti, V. P., Kubicki, J. D., Schobert, H. H. (2009). Photoinduced activation of CO_2 on Ti-based heterogeneous catalysts: Current state, chemical physics-based insights and outlook. Energy Environ Sci, 2, 745-758.

[52] Roy, S. C., Varghese, O. K., Paulose, M., Grimes, C. A. (2010). Toward solar fuels: photocatalytic conversion of carbon dioxide to hydrocarbons. ACS nano, 4, 1259-1278.

[53] Dhakshinamoorthy, A., Navalon, S., Corma, A., Garcia, H. (2012). Photocatalytic CO_2 reduction by TiO 2 and related titanium containing solids. Energy Environ Sci, 5, 9217-9233.

[54] Neațu, Ș., Maciá-Agulló, J. A., Concepción, P., Garcia, H. (2014). Gold–Copper Nanoalloys Supported on TiO_2 as Photocatalysts for CO_2 Reduction by Water. J Am Chem Soc, 136, 15969-15976.

[55] Wang, Y., He, D., Chen, H., Wang, D. (2019). Catalysts in electro-, photo-and photoelectrocatalytic CO_2 reduction reactions. Journal of Photochemistry and Photobiology C: Photochemistry Reviews, 40, 117-149.

[56] Yamazaki, Y., Takeda, H., Ishitani, O. (2015). Photocatalytic reduction of CO_2 using metal complexes. Journal of Photochemistry and Photobiology C: Photochemistry Reviews, 25, 106-137.

[57] Núñez, J., Víctor, A., Jana, P., Coronado, J. M., Serrano, D. P. (2013). Effect of copper on the performance of ZnO and ZnO_1− xNx oxides as CO_2 photoreduction catalysts. Catal Today, 209, 21-27.

[58] Khalil, M., Gunlazuardi, J., Ivandini, T. A., Umar, A. (2019). Photocatalytic conversion of CO_2 using earth-abundant catalysts: A review on mechanism and catalytic performance. Renewable and Sustainable Energy Reviews, 113, 109246.

[59] Long, R., Li, Y., Liu, Y., Chen, S., Zheng, X., Gao, C., He, C., Chen, N., Qi, Z., Song, L. (2017). Isolation of Cu atoms in Pd lattice: forming highly selective sites for photocatalytic conversion of CO_2 to CH4. J Am Chem Soc, 139, 4486-4492.

[60] An, X., Li, K., Tang, J. (2014). Cu_2O/reduced graphene oxide composites for the photocatalytic conversion of CO_2. ChemSusChem, 7, 1086-1093.

[61] Li, H., Zhang, X., MacFarlane, D. R. (2015). Carbon quantum dots/Cu_2O heterostructures for solar-light-driven conversion of CO_2 to methanol. Advanced Energy Materials, 5, 1401077.

[62] Nolan, M., Elliott, S. D. (2006). The p-type conduction mechanism in Cu 2 O: a first principles study. Phys Chem Chem Phys, 8, 5350-5358.

[63] Bi, F., Ehsan, M. F., Liu, W., He, T. (2015). Visible-Light Photocatalytic Conversion of Carbon Dioxide into Methane Using Cu_2O/TiO_2 Hollow Nanospheres. Chin J Chem, 33, 112-118.

[64] Gusain, R., Kumar, P., Sharma, O. P., Jain, S. L., Khatri, O. P. (2016). Reduced graphene oxide–CuO nanocomposites for photocatalytic conversion of CO_2 into methanol under visible light irradiation. Appl Catal B: Environ, 181, 352-362.

[65] Paracchino, A., Laporte, V., Sivula, K., Grätzel, M., Thimsen, E. (2011). Highly active oxide photocathode for photoelectrochemical water reduction. Nat Mater, 10, 456-461.

[66] Foo, W. J., Zhang, C., Ho, G. W. (2013). Non-noble metal Cu-loaded TiO 2 for enhanced photocatalytic H 2 production. Nanoscale, 5, 759-764.

[67] Tahir, M., Amin, N. S. (2015). Photocatalytic CO_2 reduction with H2 as reductant over copper and indium co-doped TiO_2 nanocatalysts in a monolith photoreactor. Appl Catal A: Gen, 493, 90-102.

[68] Tian, J., Li, H., Xing, Z., Wang, L., Luo, Y., Asiri, A. M., Al-Youbi, A. O., Sun, X. (2012). One-pot green hydrothermal synthesis of CuO–Cu 2 O–Cu nanorod-decorated reduced graphene oxide composites and their application in photocurrent generation. Catal Sci Technol, 2, 2227-2230.

[69] Tseng, I.-H., Chang, W.-C., Wu, J. C. (2002). Photoreduction of CO_2 using sol–gel derived titania and titania-supported copper catalysts. Appl Catal B: Environ, 37, 37-48.

[70] Slamet, N. H., Purnama, E., Kosela, S., Gunlazuardi, J. (2005). Photocatalytic reduction of CO_2 on copper-doped titania catalysts prepared by improved-impregnation method. Catal Commun, 6, 313-319.

[71] Li, Y., Wang, W.-N., Zhan, Z., Woo, M.-H., Wu, C.-Y., Biswas, P. (2010). Photocatalytic reduction of CO_2 with H_2O on mesoporous silica supported Cu/TiO_2 catalysts. Appl Catal B: Environ, 100, 386-392.

[72] Guan, G., Kida, T., Harada, T., Isayama, M., Yoshida, A. (2003). Photoreduction of carbon dioxide with water over $K_2Ti_6O_{13}$ photocatalyst combined with Cu/ZnO catalyst under concentrated sunlight. Appl Catal A: Gen, 249, 11-18.

[73] Wu, J., Huang, Y., Ye, W., Li, Y. (2017). CO_2 reduction: from the electrochemical to photochemical approach. Advanced Science, 4, 1700194.

[74] Xiang, Q., Cheng, B., Yu, J. (2015). Graphene-based photocatalysts for solar-fuel generation. Angew Chem Int Ed, 54, 11350-11366.

[75] Li, X., Wen, J., Low, J., Fang, Y., Yu, J. (2014). Design and fabrication of semiconductor photocatalyst for photocatalytic reduction of CO_2 to solar fuel. Science China Materials, 57, 70-100.

[76] Stolarczyk, J. K., Bhattacharyya, S., Polavarapu, L., Feldmann, J. (2018). Challenges and prospects in solar water splitting and CO_2 reduction with inorganic and hybrid nanostructures. ACS Catal, 8, 3602-3635.

[77] Tu, W., Zhou, Y., Zou, Z. (2014). Photocatalytic conversion of CO_2 into renewable hydrocarbon fuels: state-of-the-art accomplishment, challenges, and prospects. Adv Mater, 26, 4607-4626.

[78] Kisch, H. (2013). Semiconductor photocatalysis—mechanistic and synthetic aspects. Angew Chem Int Ed, 52, 812-847.

[79] Sutin, N., Creutz, C., Fujita, E. (1997). Photo-induced generation of dihydrogen and reduction of carbon dioxide using transition metal complexes. Comments Inorg Chem, 19, 67-92.

[80] Low, J., Cheng, B., Yu, J. (2017). Surface modification and enhanced photocatalytic CO_2 reduction performance of TiO_2: a review. Appl Surf Sci, 392, 658-686.

[81] Huang, Q., Yu, J., Cao, S., Cui, C., Cheng, B. (2015). Efficient photocatalytic reduction of CO_2 by amine-functionalized g-C_3N_4. Appl Surf Sci, 358, 350-355.

[82] Neaţu, S. t., Maciá-Agulló, J. A., Concepción, P., Garcia, H. (2014). Gold–copper nanoalloys supported on TiO_2 as photocatalysts for CO_2 reduction by water. J Am Chem Soc, 136, 15969-15976.

[83] White, J. L., Baruch, M. F., Pander III, J. E., Hu, Y., Fortmeyer, I. C., Park, J. E., Zhang, T., Liao, K., Gu, J., Yan, Y. (2015). Light-driven heterogeneous reduction of carbon dioxide: photocatalysts and photoelectrodes. Chem Rev, 115, 12888-12935.

[84] Kang, Q., Wang, T., Li, P., Liu, L., Chang, K., Li, M., Ye, J. (2015). Photocatalytic reduction of carbon dioxide by hydrous hydrazine over Au–Cu alloy nanoparticles supported on $SrTiO_3/TiO_2$ coaxial nanotube arrays. Angew Chem, 127, 855-859.

[85] Wang, T., Meng, X., Li, P., Ouyang, S., Chang, K., Liu, G., Mei, Z., Ye, J. (2014). Photoreduction of CO_2 over the well-crystallized ordered mesoporous TiO_2 with the confined space effect. Nano Energy, 9, 50-60.

[86] Raciti, D., Wang, C. (2018). Recent advances in CO_2 reduction electrocatalysis on copper. ACS Energy Letters, 3, 1545-1556.

[87] Agarwal, A. S., Rode, E., Sridhar, N., Hill, D. (2017). Conversion of CO_2 to value-added chemicals: Opportunities and challenges. Handbook of climate change mitigation and adaptation Cham: Springer International Publishing, 2487-2526.

[88] Xie, J., Huang, Y., Wu, M., Wang, Y. (2019). Electrochemical carbon dioxide splitting. ChemElectroChem, 6, 1587-1604.

[89] Hori, Y., Takahashi, R., Yoshinami, Y., Murata, A. (1997). Electrochemical reduction of CO at a copper electrode. J Phys Chem B, 101, 7075-7081.

[90] Nitopi, S., Bertheussen, E., Scott, S. B., Liu, X., Engstfeld, A. K., Horch, S., Seger, B., Stephens, I. E., Chan, K., Hahn, C. (2019). Progress and perspectives of electrochemical CO_2 reduction on copper in aqueous electrolyte. Chem Rev, 119, 7610-7672.

[91] Yang, Y., Ohnoutek, L., Ajmal, S., Zheng, X., Feng, Y., Li, K., Wang, T., Deng, Y., Liu, Y., Xu, D. (2019). "Hot edges" in an inverse opal structure enable efficient CO_2 electrochemical reduction and sensitive in situ Raman characterization. J Mater Chem A, 7, 11836-11846.

[92] Kortlever, R., Shen, J., Schouten, K. J. P., Calle-Vallejo, F., Koper, M. T. (2015). Catalysts and reaction pathways for the electrochemical reduction of carbon dioxide. The journal of physical chemistry letters, 6, 4073-4082.

[93] Hori, Y., Wakebe, H., Tsukamoto, T., Koga, O. (1994). Electrocatalytic process of CO selectivity in electrochemical reduction of CO_2 at metal electrodes in aqueous media. Electrochim Acta, 39, 1833-1839.

[94] Garza, A. J., Bell, A. T., Head-Gordon, M. (2018). Mechanism of CO_2 reduction at copper surfaces: pathways to C2 products. ACS Catal, 8, 1490-1499.

[95] Lin, S.-C., Chang, C.-C., Chiu, S.-Y., Pai, H.-T., Liao, T.-Y., Hsu, C.-S., Chiang, W.-H., Tsai, M.-K., Chen, H. M. (2020). Operando time-resolved X-ray absorption spectroscopy reveals the chemical nature enabling highly selective CO_2 reduction. Nat Commun, 11, 1-12.

[96] Ren, D., Deng, Y., Handoko, A. D., Chen, C. S., Malkhandi, S., Yeo, B. S. (2015). Selective electrochemical reduction of carbon dioxide to ethylene and ethanol on copper (I) oxide catalysts. ACS Catal, 5, 2814-2821.

[97] Chen, C. S., Handoko, A. D., Wan, J. H., Ma, L., Ren, D., Yeo, B. S. (2015). Stable and selective electrochemical reduction of carbon dioxide to ethylene on copper mesocrystals. Catal Sci Technol, 5, 161-168.

[98] Kuhl, K. P., Cave, E. R., Abram, D. N., Jaramillo, T. F. (2012). New insights into the electrochemical reduction of carbon dioxide on metallic copper surfaces. Energy Environ Sci, 5, 7050-7059.

[99] Feng, X., Jiang, K., Fan, S., Kanan, M. W. (2016). A direct grain-boundary-activity correlation for CO electroreduction on Cu nanoparticles. ACS Cent Sci, 2, 169-174.

[100] Nie, X., Esopi, M. R., Janik, M. J., Asthagiri, A. (2013). Selectivity of CO_2 reduction on copper electrodes: the role of the kinetics of elementary steps. Angew Chem, 125, 2519-2522.

[101] Hori, Y., Takahashi, I., Koga, O., Hoshi, N. (2003). Electrochemical reduction of carbon dioxide at various series of copper single crystal electrodes. J Mol Catal A: Chem, 199, 39-47.

[102] Hori, Y., Wakebe, H., Tsukamoto, T., Koga, O. (1995). Adsorption of CO accompanied with simultaneous charge transfer on copper single crystal electrodes related with electrochemical reduction of CO_2 to hydrocarbons. Surf Sci, 335, 258-263.

[103] Dattila, F., García-Muelas, R., López, N. (2020). Active and Selective Ensembles in Oxide-Derived Copper Catalysts for CO_2 Reduction. ACS Energy Letters, 5, 3176-3184.

[104] Hori, Y., Murata, A., Takahashi, R., Suzuki, S. (1987). Electroreduction of carbon monoxide to methane and ethylene at a copper electrode in aqueous solutions at ambient temperature and pressure. J Am Chem Soc, 109, 5022-5023.

[105] Hansen, H. A., Varley, J. B., Peterson, A. A., Nørskov, J. K. (2013). Understanding trends in the electrocatalytic activity of metals and enzymes for CO_2 reduction to CO. The journal of physical chemistry letters, 4, 388-392.

[106] Schouten, K., Kwon, Y., Van der Ham, C., Qin, Z., Koper, M. (2011). A new mechanism for the selectivity to C 1 and C 2 species in the electrochemical reduction of carbon dioxide on copper electrodes. Cheml Sci, 2, 1902-1909.

[107] Calle-Vallejo, F., Koper, M. T. (2013). Theoretical considerations on the electroreduction of CO to C2 species on Cu (100) electrodes. Angew Chem, 125, 7423-7426.

[108] Cheng, T., Xiao, H., Goddard, W. A. (2017). Full atomistic reaction mechanism with kinetics for CO reduction on Cu (100) from ab initio molecular dynamics free-energy calculations at 298 K. Proc Natl Acad Sci, 114, 1795-1800.

[109] Goodpaster, J. D., Bell, A. T., Head-Gordon, M. (2016). Identification of possible pathways for C–C bond formation during electrochemical reduction of CO_2: new theoretical insights from an improved electrochemical model. The journal of physical chemistry letters, 7, 1471-1477.

[110] Luo, W., Nie, X., Janik, M. J., Asthagiri, A. (2016). Facet Dependence of CO_2 Reduction Paths on Cu Electrodes. ACS Catal, 6, 219-229.

[111] Koper, M. T. (2013). Theory of multiple proton–electron transfer reactions and its implications for electrocatalysis. Cheml Sci, 4, 2710-2723.

[112] Cheng, T., Fortunelli, A., Goddard, W. A. (2019). Reaction intermediates during operando electrocatalysis identified from full solvent quantum mechanics molecular dynamics. Proc Natl Acad Sci, 116, 7718-7722.

[113] Cheng, T., Xiao, H., Goddard III, W. A. (2016). Reaction mechanisms for the electrochemical reduction of CO_2 to CO and formate on the Cu (100) surface at 298 K from quantum mechanics free energy calculations with explicit water. J Am Chem Soc, 138, 13802-13805.

[114] Heyes, J., Dunwell, M., Xu, B. (2016). CO_2 reduction on Cu at low overpotentials with surface-enhanced in situ spectroscopy. J Phy Chem C, 120, 17334-17341.

[115] Figueiredo, M. C., Ledezma-Yanez, I., Koper, M. T. (2016). In situ spectroscopic study of CO_2 electroreduction at copper electrodes in acetonitrile. ACS Catal, 6, 2382-2392.

[116] Zhu, S., Jiang, B., Cai, W.-B., Shao, M. (2017). Direct observation on reaction intermediates and the role of bicarbonate anions in CO_2 electrochemical reduction reaction on Cu surfaces. J Am Chem Soc, 139, 15664-15667.

[117] Gunathunge, C. M., Li, X., Li, J., Hicks, R. P., Ovalle, V. J., Waegele, M. M. (2017). Spectroscopic observation of reversible surface reconstruction of copper electrodes under CO_2 reduction. J Phy Chem C, 121, 12337-12344.

[118] Moradzaman, M., Mul, G. (2020). Infrared Analysis of Interfacial Phenomena during Electrochemical Reduction of CO_2 over Polycrystalline Copper Electrodes. ACS Catal, 10, 8049-8057.

[119] Gawande, M. B., Goswami, A., Felpin, F.-X., Asefa, T., Huang, X., Silva, R., Zou, X., Zboril, R., Varma, R. S. (2016). Cu and Cu-based nanoparticles: synthesis and applications in catalysis. Chem Rev, 116, 3722-3811.

[120] Jeon, H. S., Timoshenko, J., Scholten, F., Sinev, I., Herzog, A., Haase, F. T., Roldan Cuenya, B. (2019). Operando Insight into the Correlation between the Structure and Composition of CuZn Nanoparticles and their Selectivity for the Electrochemical CO_2 Reduction. J Am Chem Soc, 141, 19879-19887.

[121] Ma, Z., Tsounis, C., Kumar, P. V., Han, Z., Wong, R. J., Toe, C. Y., Zhou, S., Bedford, N. M., Thomsen, L., Ng, Y. H. (2020). Enhanced Electrochemical CO_2 Reduction of Cu@ CuxO Nanoparticles Decorated on 3D Vertical Graphene with Intrinsic sp3-type Defect. Adv Funct Mater, 1910118.

[122] Ament, K., Köwitsch, N., Hou, D., Götsch, T., Kröhnert, J., Heard, C. J., Trunschke, A., Lunkenbein, T., Armbrüster, M., Breu, J. (2020). Nanoparticles Supported on Sub-Nanometer Oxide Films: Scaling Model Systems to Bulk Materials. Angew Chem Int Ed.

[123] Larmier, K., Liao, W. C., Tada, S., Lam, E., Verel, R., Bansode, A., Urakawa, A., Comas-Vives, A., Copéret, C. (2017). CO_2-to-methanol hydrogenation on zirconia-supported copper nanoparticles: reaction intermediates and the role of the metal–support interface. Angew Chem Int Ed, 56, 2318-2323.

[124] Wu, Y. A., McNulty, I., Liu, C., Lau, K. C., Liu, Q., Paulikas, A. P., Sun, C.-J., Cai, Z., Guest, J. R., Ren, Y. (2019). Facet-dependent active sites of a single Cu_2O particle photocatalyst for CO_2 reduction to methanol. Nature Energy, 4, 957-968.

[125] Frei, E., Gaur, A., Lichternberg, H., Zwiener, L., Scherzer, M., Girgsdies, F., Lunkenbein, T., Schlögl, R. (2020). Cu− Zn Alloy Formation as Unfavored State for Efficient Methanol Catalysts. ChemCatChem, 12, 4029-4033.

[126] Lam, E., Noh, G., Chan, K. W., Larmier, K., Lebedev, D., Searles, K., Wolf, P., Safonova, O. V., Copéret, C. (2020). Enhanced CH 3 OH selectivity in CO_2 hydrogenation using Cu-based catalysts generated via SOMC from Ga III single-sites. Cheml Sci, 11, 7593-7598.

[127] Manrique, R., Rodríguez-Pereira, J., Rincón-Ortiz, S. A., Bravo-Suárez, J. J., Baldovino-Medrano, V. G., Jiménez, R., Karelovic, A. (2020). The nature of the active sites of Pd–Ga catalysts in the hydrogenation of CO_2 to methanol. Catal Sci Technol, 10, 6644-6658.

[128] Li, C. W., Ciston, J., Kanan, M. W. (2014). Electroreduction of carbon monoxide to liquid fuel on oxide-derived nanocrystalline copper. Nature, 508, 504-507.

[129] Handoko, A. D., Chan, K. W., Yeo, B. S. (2017). –CH3 mediated pathway for the electroreduction of CO_2 to ethane and ethanol on thick oxide-derived copper catalysts at low overpotentials. ACS Energy Letters, 2, 2103-2109.

[130] Scott, S. B., Hogg, T. V., Landers, A. T., Maagaard, T., Bertheussen, E., Lin, J. C., Davis, R. C., Beeman, J. W., Higgins, D., Drisdell, W. S. (2019). Absence of oxidized phases in Cu under CO reduction conditions. ACS Energy Letters, 4, 803-804.

[131] Zhu, Q., Sun, X., Yang, D., Ma, J., Kang, X., Zheng, L., Zhang, J., Wu, Z., Han, B. (2019). Carbon dioxide electroreduction to C 2 products over copper-cuprous oxide derived from electrosynthesized copper complex. Nat Commun, 10, 1-11.

[132] Chang, X., Wang, T., Zhang, P., Wei, Y., Zhao, J., Gong, J. (2016). Stable aqueous photoelectrochemical CO_2 reduction by a Cu_2O dark cathode with improved selectivity for carbonaceous products. Angew Chem Int Ed, 55, 8840-8845.

[133] Chang, X., Wang, T., Zhang, P., Wei, Y., Zhao, J., Gong, J. (2016). Frontispiece: Stable Aqueous Photoelectrochemical CO_2 Reduction by a Cu_2O Dark Cathode with Improved Selectivity for Carbonaceous Products. Angew Chem Int Ed, 55.

[134] Dutta, A., Rahaman, M., Luedi, N. C., Mohos, M., Broekmann, P. (2016). Morphology matters: tuning the product distribution of CO_2 electroreduction on oxide-derived Cu foam catalysts. ACS Catal, 6, 3804-3814.

[135] Li, J., Che, F., Pang, Y., Zou, C., Howe, J. Y., Burdyny, T., Edwards, J. P., Wang, Y., Li, F., Wang, Z. (2018). Copper adparticle enabled selective electrosynthesis of n-propanol. Nat Commun, 9, 1-9.

[136] Ting, L. R. L., García-Muelas, R., Martín, A. J., Veenstra, F. L., Chen, S. T. J., Peng, Y., Per, E. Y. X., Pablo-García, S., López, N., Pérez-Ramírez, J. (2020). Electrochemical Reduction of Carbon Dioxide to 1-Butanol on Oxide-Derived Copper. Angew Chem, 132, 21258-21265.

[137] Eilert, A., Cavalca, F., Roberts, F. S., Osterwalder, J. r., Liu, C., Favaro, M., Crumlin, E. J., Ogasawara, H., Friebel, D., Pettersson, L. G. (2017). Subsurface oxygen in oxide-derived copper electrocatalysts for carbon dioxide reduction. The journal of physical chemistry letters, 8, 285-290.

[138] Li, C. W., Kanan, M. W. (2012). CO_2 reduction at low overpotential on Cu electrodes resulting from the reduction of thick Cu_2O films. J Am Chem Soc, 134, 7231-7234.

[139] Zhuang, T.-T., Pang, Y., Liang, Z.-Q., Wang, Z., Li, Y., Tan, C.-S., Li, J., Dinh, C. T., De Luna, P., Hsieh, P.-L. (2018). Copper nanocavities confine intermediates for efficient electrosynthesis of C3 alcohol fuels from carbon monoxide. Nat Catal, 1, 946-951.

[140] Chang, X., Malkani, A., Yang, X., Xu, B. (2020). Mechanistic Insights into Electroreductive C–C coupling between CO and acetaldehyde into multicarbon products. J Am Chem Soc, 142, 2975-2983.

[141] Verdaguer-Casadevall, A., Li, C. W., Johansson, T. P., Scott, S. B., McKeown, J. T., Kumar, M., Stephens, I. E., Kanan, M. W., Chorkendorff, I. (2015). Probing the active surface sites for CO reduction on oxide-derived copper electrocatalysts. J Am Chem Soc, 137, 9808-9811.

[142] Bertheussen, E., Hogg, T. V., Abghoui, Y., Engstfeld, A. K., Chorkendorff, I., Stephens, I. E. (2018). Electroreduction of CO on polycrystalline copper at low overpotentials. ACS Energy Letters, 3, 634-640.

[143] Greeley, J. P. (2012). Active Site of an Industrial Catalyst. Science, 336, 810.

[144] Pan, Y., Shen, X., Yao, L., Bentalib, A., Peng, Z. (2018). Active sites in heterogeneous catalytic reaction on metal and metal oxide: theory and practice. Catalysts, 8, 478.

[145] Li, Y., Chan, S. H., Sun, Q. (2015). Heterogeneous catalytic conversion of CO_2: a comprehensive theoretical review. Nanoscale, 7, 8663-8683.

[146] Tada, S., Kayamori, S., Honma, T., Kamei, H., Nariyuki, A., Kon, K., Toyao, T., Shimizu, K.-i., Satokawa, S. (2018). Design of interfacial sites between Cu and amorphous ZrO_2 dedicated to CO_2-to-Methanol hydrogenation. ACS Catal, 8, 7809-7819.

[147] Cheng, T., Xiao, H., Goddard, W. A. (2017). Nature of the Active Sites for CO Reduction on Copper Nanoparticles; Suggestions for Optimizing Performance. J Am Chem Soc, 139, 11642-11645.

[148] Peterson, A. A., Abild-Pedersen, F., Studt, F., Rossmeisl, J., Nørskov, J. K. (2010). How copper catalyzes the electroreduction of carbon dioxide into hydrocarbon fuels. Energy Environ Sci, 3, 1311-1315.

[149] Liu, S., Huang, S. (2019). Size effects and active sites of Cu nanoparticle catalysts for CO_2 electroreduction. Appl Surf Sci, 475, 20-27.

[150] Chen, C., Yan, X., Wu, Y., Liu, S., Sun, X., Zhu, Q., Feng, R., Wu, T., Qian, Q., Liu, H., Zheng, L., Zhang, J., Han, B. (2021). The in situ study of surface species and structures of oxide-derived copper catalysts for electrochemical CO_2 reduction. Cheml Sci.

[151] Mistry, H., Varela, A. S., Bonifacio, C. S., Zegkinoglou, I., Sinev, I., Choi, Y.-W., Kisslinger, K., Stach, E. A., Yang, J. C., Strasser, P., Cuenya, B. R. (2016). Highly selective plasma-activated copper catalysts for carbon dioxide reduction to ethylene. Nat Commun, 7, 12123.

[152] Tisseraud, C., Comminges, C., Belin, T., Ahouari, H., Soualah, A., Pouilloux, Y., Le Valant, A. (2015). The Cu–ZnO synergy in methanol synthesis from CO_2, Part 2: Origin of the methanol and CO selectivities explained by experimental studies and a sphere contact quantification model in randomly packed binary mixtures on Cu–ZnO coprecipitate catalysts. J Catal, 330, 533-544.

[153] Greeley, J., Nørskov, J. K., Mavrikakis, M. (2002). Electronic structure and catalysis on metal surfaces. Annu Rev Phys Chem, 53, 319-348.

[154] Somorjai, G. A., Li, Y. (2010) Introduction to surface chemistry and catalysis, John Wiley & Sons.

[155] Choi, Y., Futagami, K., Fujitani, T., Nakamura, J. (2001). The difference in the active sites for CO_2 and CO hydrogenations on Cu/ZnO-based methanol synthesis catalysts. Catal Lett, 73, 27-31.

[156] Gao, P., Li, F., Xiao, F., Zhao, N., Sun, N., Wei, W., Zhong, L., Sun, Y. (2012). Preparation and activity of Cu/Zn/Al/Zr catalysts via hydrotalcite-containing precursors for methanol synthesis from CO_2 hydrogenation. Catal Sci Technol, 2, 1447-1454.

[157] Behrens, M., Studt, F., Kasatkin, I., Kühl, S., Hävecker, M., Abild-Pedersen, F., Zander, S., Girgsdies, F., Kurr, P., Kniep, B.-L. (2012). The active site of methanol synthesis over $Cu/ZnO/Al_2O_3$ industrial catalysts. Science, 336, 893-897.

[158] Zander, S., Kunkes, E. L., Schuster, M. E., Schumann, J., Weinberg, G., Teschner, D., Jacobsen, N., Schlögl, R., Behrens, M. (2013). The role of the oxide component in the development of copper composite catalysts for methanol synthesis. Angew Chem Int Ed, 52, 6536-6540.

[159] Kunkes, E. L., Studt, F., Abild-Pedersen, F., Schlögl, R., Behrens, M. (2015). Hydrogenation of CO_2 to methanol and CO on $Cu/ZnO/Al_2O_3$: Is there a common intermediate or not? J Catal, 328, 43-48.

[160] Dasireddy, V. D., Likozar, B. (2019). The role of copper oxidation state in $Cu/ZnO/Al_2O_3$ catalysts in CO_2 hydrogenation and methanol productivity. Renew Energ, 140, 452-460.

[161] Fujitani, T., Nakamura, I., Watanabe, T., Uchijima, T., Nakamura, J. (1995). Methanol synthesis by the hydrogenation of CO_2 over Zn-deposited Cu (111) and Cu (110) surfaces. Catal Lett, 35, 297-302.

[162] Yao, L., Shen, X., Pan, Y., Peng, Z. (2019). Synergy between active sites of Cu-In-Zr-O catalyst in CO_2 hydrogenation to methanol. J Catal, 372, 74-85.

[163] Kuld, S., Thorhauge, M., Falsig, H., Elkjær, C. F., Helveg, S., Chorkendorff, I., Sehested, J. (2016). Quantifying the promotion of Cu catalysts by ZnO for methanol synthesis. Science, 352, 969-974.

[164] Kattel, S., Ramírez, P. J., Chen, J. G., Rodriguez, J. A., Liu, P. (2017). Active sites for CO_2 hydrogenation to methanol on Cu/ZnO catalysts. Science, 355, 1296-1299.

[165] Le Valant, A., Comminges, C., Tisseraud, C., Canaff, C., Pinard, L., Pouilloux, Y. (2015). The Cu–ZnO synergy in methanol synthesis from CO_2, Part 1: Origin of active site explained by experimental studies and a sphere contact quantification model on Cu+ ZnO mechanical mixtures. J Catal, 324, 41-49.

[166] Graciani, J., Mudiyanselage, K., Xu, F., Baber, A. E., Evans, J., Senanayake, S. D., Stacchiola, D. J., Liu, P., Hrbek, J., Sanz, J. F. (2014). Highly active copper-ceria and copper-ceria-titania catalysts for methanol synthesis from CO_2. Science, 345, 546-550.

[167] Kanai, Y., Watanabe, T., Fujitani, T., Saito, M., Nakamura, J., Uchijima, T. (1994). Evidence for the migration of ZnO x in a Cu/ZnO methanol synthesis catalyst. Catal Lett, 27, 67-78.

[168] Yoshihara, J., Campbell, C. T. (1996). Methanol synthesis and reverse water–gas shift kinetics over Cu (110) model catalysts: structural sensitivity. J Catal, 161, 776-782.

[169] Yoshihara, J., Parker, S., Schafer, A., Campbell, C. T. (1995). Methanol synthesis and reverse water-gas shift kinetics over clean polycrystalline copper. Catal Lett, 31, 313-324.

[170] Gao, J., Song, F., Li, Y., Cheng, W., Yuan, H., Xu, Q. (2020). Cu_2In nanoalloy enhanced performance of Cu/ZrO_2 catalysts for the CO_2 hydrogenation to methanol. Ind Eng Chem Res.

[171] Kas, R., Kortlever, R., Milbrat, A., Koper, M. T., Mul, G., Baltrusaitis, J. (2014). Electrochemical CO_2 reduction on Cu 2 O-derived copper nanoparticles: controlling the catalytic selectivity of hydrocarbons. Phys Chem Chem Phys, 16, 12194-12201.

[172] Ren, D., Wong, N. T., Handoko, A. D., Huang, Y., Yeo, B. S. (2016). Mechanistic insights into the enhanced activity and stability of agglomerated Cu nanocrystals for the electrochemical reduction of carbon dioxide to n-propanol. The journal of physical chemistry letters, 7, 20-24.

[173] Mandal, L., Yang, K. R., Motapothula, M. R., Ren, D., Lobaccaro, P., Patra, A., Sherburne, M., Batista, V. S., Yeo, B. S., Ager, J. W., Martin, J., Venkatesan, T. (2018). Investigating the Role of Copper Oxide in Electrochemical CO_2 Reduction in Real Time. ACS Appl Mater Interfaces, 10, 8574-8584.

[174] Weng, Z., Wu, Y., Wang, M., Jiang, J., Yang, K., Huo, S., Wang, X.-F., Ma, Q., Brudvig, G. W., Batista, V. S. (2018). Active sites of copper-complex catalytic materials for electrochemical carbon dioxide reduction. Nat Commun, 9, 1-9.

[175] Nielsen, N. D., Smitshuysen, T. E., Damsgaard, C. D., Jensen, A. D., Christensen, J. M. (2021). Characterization of oxide-supported Cu by infrared measurements on adsorbed CO. Surf Sci, 703, 121725.

[176] Kanai, Y., Watanabe, T., Fujitani, T., Uchijima, T., Nakamura, J. (1996). The synergy between Cu and ZnO in methanol synthesis catalysts. Catal Lett, 38, 157-163.

[177] Laudenschleger, D., Ruland, H., Muhler, M. (2020). Identifying the nature of the active sites in methanol synthesis over Cu/ZnO/Al 2 O 3 catalysts. Nat Commun, 11, 1-10.

[178] Jiang, X., Wang, X., Nie, X., Koizumi, N., Guo, X., Song, C. (2018). CO_2 hydrogenation to methanol on Pd-Cu bimetallic catalysts: H_2/CO_2 ratio dependence and surface species. Catal Today, 316, 62-70.

[179] Jiang, X., Nie, X., Wang, X., Wang, H., Koizumi, N., Chen, Y., Guo, X., Song, C. (2019). Origin of Pd-Cu bimetallic effect for synergetic promotion of methanol formation from CO_2 hydrogenation. J Catal, 369, 21-32.

[180] Wang, W., Qu, Z., Song, L., Fu, Q. (2020). Probing into the multifunctional role of copper species and reaction pathway on copper-cerium-zirconium catalysts for CO_2 hydrogenation to methanol using high pressure in situ DRIFTS. J Catal, 382, 129-140.

[181] Rasul, S., Anjum, D. H., Jedidi, A., Minenkov, Y., Cavallo, L., Takanabe, K. (2015). A highly selective copper–indium bimetallic electrocatalyst for the electrochemical reduction of aqueous CO_2 to CO. Angew Chem, 127, 2174-2178.

[182] Samson, K., Sliwa, M., Socha, R. P., Góra-Marek, K., Mucha, D., Rutkowska-Zbik, D., Paul, J., Ruggiero-Mikołajczyk, M., Grabowski, R., Słoczynski, J. (2014). Influence of ZrO_2 structure and copper electronic state on activity of Cu/ZrO_2 catalysts in methanol synthesis from CO_2. ACS Catal, 4, 3730-3741.

[183] Ro, I., Liu, Y., Ball, M. R., Jackson, D. H., Chada, J. P., Sener, C., Kuech, T. F., Madon, R. J., Huber, G. W., Dumesic, J. A. (2016). Role of the $Cu-ZrO_2$ interfacial sites for conversion of ethanol to ethyl acetate and synthesis of methanol from CO_2 and H2. ACS Catal, 6, 7040-7050.

[184] Lam, E., Larmier, K., Wolf, P., Tada, S., Safonova, O. V., Copéret, C. (2018). Isolated Zr surface sites on silica promote hydrogenation of CO_2 to CH_3OH in supported Cu catalysts. J Am Chem Soc, 140, 10530-10535.

[185] Lam, E., Corral-Pérez, J. J., Larmier, K., Noh, G., Wolf, P., Comas-Vives, A., Urakawa, A., Copéret, C. (2019). CO_2 hydrogenation on Cu/Al_2O_3: Role of the metal/support interface in driving activity and selectivity of a bifunctional catalyst. Angew Chem, 131, 14127-14134.

[186] Zheng, H., Narkhede, N., Han, L., Zhang, H., Li, Z. (2020). Methanol synthesis from CO_2: a DFT investigation on Zn-promoted Cu catalyst. Res Chem Intermed, 46, 1749-1769.

[187] Chang, X., Wang, T., Zhao, Z. J., Yang, P., Greeley, J., Mu, R., Zhang, G., Gong, Z., Luo, Z., Chen, J. (2018). Tuning Cu/Cu_2O interfaces for the reduction of carbon dioxide to methanol in aqueous solutions. Angew Chem Int Ed, 57, 15415-15419.

[188] Chen, K., Fang, H., Wu, S., Liu, X., Zheng, J., Zhou, S., Duan, X., Zhuang, Y., Tsang, S. C. E., Yuan, Y. (2019). CO_2 hydrogenation to methanol over Cu catalysts supported on La-modified SBA-15: The crucial role of Cu–LaOx interfaces. Appl Catal B: Environ, 251, 119-129.

[189] Hong, Q.-J., Liu, Z.-P. (2010). Mechanism of CO_2 hydrogenation over Cu/ZrO_2 (212) interface from first-principles kinetics Monte Carlo simulations. Surf Sci, 604, 1869-1876.

[190] Tang, Q.-L., Hong, Q.-J., Liu, Z.-P. (2009). CO_2 fixation into methanol at Cu/ZrO_2 interface from first principles kinetic Monte Carlo. J Catal, 263, 114-122.

[191] Polierer, S., Jelic, J., Pitter, S., Studt, F. (2019). On the reactivity of the Cu/ZrO_2 system for the hydrogenation of CO_2 to methanol: A density functional theory study. J Phy Chem C, 123, 26904-26911.

[192] Liu, L., Su, X., Zhang, H., Gao, N., Xue, F., Ma, Y., Jiang, Z., Fang, T. (2020). Zirconia-Modified Copper Catalyst for CO_2 Conversion to Methanol from DFT Study. Appl Surf Sci, 146900.

[193] Wang, L.-X., Guan, E., Wang, Z., Wang, L., Gong, Z., Cui, Y., Yang, Z., Wang, C., Zhang, J., Meng, X. (2020). Dispersed Nickel Boosts Catalysis by Copper in CO_2 Hydrogenation. ACS Catal, 10, 9261-9270.

[194] Herman, R., Klier, K., Simmons, G., Finn, B., Bulko, J. B., Kobylinski, T. (1979). Catalytic synthesis of methanol from COH_2:I. Phase composition, electronic properties, and activities of the $Cu/ZnO/M_2O_3$ catalysts. J Catal, 56, 407-429.

[195] Chu, S., Yan, X., Choi, C., Hong, S., Robertson, A. W., Masa, J., Han, B., Jung, Y., Sun, Z. (2020). Stabilization of Cu+ by tuning a CuO–CeO 2 interface for selective electrochemical CO_2 reduction to ethylene. Green Chem, 22, 6540-6546.

[196] Palomino, R. M., Ramírez, P. J., Liu, Z., Hamlyn, R., Waluyo, I., Mahapatra, M., Orozco, I., Hunt, A., Simonovis, J. P., Senanayake, S. D. (2018). Hydrogenation of CO_2 on ZnO/Cu (100) and ZnO/Cu (111) catalysts: role of copper structure and metal–oxide interface in methanol synthesis. J Phys Chem B, 122, 794-800.

[197] Zhang, Z., Wang, S.-S., Song, R., Cao, T., Luo, L., Chen, X., Gao, Y., Lu, J., Li, W.-X., Huang, W. (2017). The most active Cu facet for low-temperature water gas shift reaction. Nat Commun, 8, 1-10.

[198] Nakamura, J., Choi, Y., Fujitani, T. (2003). On the issue of the active site and the role of ZnO in Cu/ZnO methanol synthesis catalysts. Top Catal, 22, 277-285.

[199] Kuld, S., Conradsen, C., Moses, P. G., Chorkendorff, I., Sehested, J. (2014). Quantification of Zinc Atoms in a Surface Alloy on Copper in an Industrial-Type Methanol Synthesis Catalyst. Angew Chem Int Ed, 53, 5941-5945.

[200] Fichtl, M. B., Schumann, J., Kasatkin, I., Jacobsen, N., Behrens, M., Schlögl, R., Muhler, M., Hinrichsen, O. (2014). Counting of oxygen defects versus metal surface sites in methanol synthesis catalysts by different probe molecules. Angew Chem Int Ed, 53, 7043-7047.

[201] Boudart, M. (1995). Turnover rates in heterogeneous catalysis. Chem Rev, 95, 661-666.

[202] Arena, F., Mezzatesta, G., Zafarana, G., Trunfio, G., Frusteri, F., Spadaro, L. (2013). Effects of oxide carriers on surface functionality and process performance of the Cu–ZnO system in the synthesis of methanol via CO_2 hydrogenation. J Catal, 300, 141-151.

[203] Zhai, Q., Xie, S., Fan, W., Zhang, Q., Wang, Y., Deng, W., Wang, Y. (2013). Photocatalytic conversion of carbon dioxide with water into methane: platinum and copper (I) oxide co-catalysts with a core–shell structure. Angew Chem, 125, 5888-5891.

[204] Lee, S., Kim, D., Lee, J. (2015). Electrocatalytic production of C3-C4 compounds by conversion of CO_2 on a chloride-induced bi-phasic Cu_2O-Cu catalyst. Angew Chem, 127, 14914-14918.

[205] Szanyi, J., Goodman, D. W. (1991). Methanol synthesis on a Cu (100) catalyst. Catal Lett, 10, 383-390.

[206] Millar, G. J., Rochester, C. H., Bailey, S., Waugh, K. C. (1993). Combined temperature-programmed desorption and fourier-transform infrared spectroscopy study of CO_2, CO and H_2 interactions with model ZnO/SiO_2, Cu/SiO_2 and $Cu/ZnO/SiO_2$ methanol synthesis catalysts. J Chem Soc, Faraday Trans, 89, 1109-1115.

[207] Ghiotti, G., Boccuzzi, F., Chiorino, A. (1986). The operation of the “metal-surface selection rule” on the vibrational spectra of species adsorbed on supported copper particles. Surf Sci, 178, 553-564.

[208] Topsøe, N.-Y., Topsøe, H. (1999). FTIR studies of dynamic surface structural changes in Cu-based methanol synthesis catalysts. J Mol Catal A: Chem, 141, 95-105.

[209] Xue, J., Wang, X., Qi, G., Wang, J., Shen, M., Li, W. (2013). Characterization of copper species over Cu/SAPO-34 in selective catalytic reduction of NOx with ammonia: Relationships between active Cu sites and de-NOx performance at low temperature. J Catal, 297, 56-64.

[210] Padley, M. B., Rochester, C. H., Hutchings, G. J., King, F. (1994). FTIR spectroscopic study of thiophene, SO2, and CO adsorption on Cu/Al_2O_3 catalysts. J Catal, 148, 438-452.

[211] Espinós, J. P., Morales, J., Barranco, A., Caballero, A., Holgado, J., González-Elipe, A. (2002). Interface effects for Cu, CuO, and Cu_2O deposited on SiO_2 and ZrO_2. XPS determination of the valence state of copper in Cu/SiO_2 and Cu/ZrO_2 catalysts. J Phys Chem B, 106, 6921-6929.

[212] Montini, T., Gombac, V., Sordelli, L., Delgado, J. J., Chen, X., Adami, G., Fornasiero, P. (2011). Nanostructured Cu/TiO_2 Photocatalysts for H2 Production from Ethanol and Glycerol Aqueous Solutions. ChemCatChem, 3, 574-577.

[213] Bai, X., Li, Q., Shi, L., Niu, X., Ling, C., Wang, J. (2020). Hybrid CuO and Cux+ as Atomic Interfaces Promote High-Selectivity Conversion of CO_2 to C_2H_5OH at Low Potential. Small, 16, 1901981.

[214] Tseng, I.-H., Wu, J. C., Chou, H.-Y. (2004). Effects of sol–gel procedures on the photocatalysis of Cu/TiO_2 in CO_2 photoreduction. J Catal, 221, 432-440.

[215] Slamet, H. W. N., Purnama, E., Riyani, K., Gunlazuardi, J. (2009). Effect of copper species in a photocatalytic synthesis of methanol from carbon dioxide over copper-doped titania catalysts. World Applied Sciences Journal, 6, 112-122.

[216] Liu, D., Fernández, Y., Ola, O., Mackintosh, S., Maroto-Valer, M., Parlett, C. M., Lee, A. F., Wu, J. C. (2012). On the impact of Cu dispersion on CO_2 photoreduction over Cu/TiO_2. Catal Commun, 25, 78-82.

[217] Velu, S., Suzuki, K., Gopinath, C. S., Yoshida, H., Hattori, T. (2002). XPS, XANES and EXAFS investigations of CuO/ZnO/Al 2 O 3/ZrO 2 mixed oxide catalysts. Phys Chem Chem Phys, 4, 1990-1999.

[218] Moretti, G., Fierro, G., Lo Jacono, M., Porta, P. (1989). Characterization of CuO–ZnO catalysts by X-ray photoelectron spectroscopy: Precursors, calcined and reduced samples. Surf Interface Anal, 14, 325-336.

[219] Reitz, T., Lee, P., Czaplewski, K., Lang, J., Popp, K., Kung, H. (2001). Time-resolved XANES investigation of CuO/ZnO in the oxidative methanol reforming reaction. J Catal, 199, 193-201.

[220] Wang, R., Jiang, R., Dong, C., Tong, T., Li, Z., Liu, H., Du, X.-W. (2021). Engineering a Cu/ZnOx Interface for High Methane Selectivity in CO_2 Electrochemical Reduction. Ind Eng Chem Res, 60, 273-280.

[221] Schedel-Niedrig, T., Neisius, T., Böttger, I., Kitzelmann, E., Weinberg, G., Demuth, D., Schlögl, R. (2000). Copper (sub) oxide formation: a surface sensitive characterization of model catalysts. Phys Chem Chem Phys, 2, 2407-2417.

[222] Zhang, W., Huang, C., Xiao, Q., Yu, L., Shuai, L., An, P., Zhang, J., Qiu, M., Ren, Z., Yu, Y. (2020). Atypical oxygen-bearing copper boosts ethylene selectivity toward electrocatalytic CO_2 reduction. J Am Chem Soc, 142, 11417-11427.

[223] Arán-Ais, R. M., Scholten, F., Kunze, S., Rizo, R., Cuenya, B. R. (2020). The role of in situ generated morphological motifs and Cu (i) species in C2+ product selectivity during CO_2 pulsed electroreduction. Nature Energy, 5, 317-325.

[224] Gao, D., Arán-Ais, R. M., Jeon, H. S., Cuenya, B. R. (2019). Rational catalyst and electrolyte design for CO_2 electroreduction towards multicarbon products. Nat Catal, 2, 198-210.

[225] Lum, Y., Ager, J. W. (2019). Evidence for product-specific active sites on oxide-derived Cu catalysts for electrochemical CO_2 reduction. Nat Catal, 2, 86-93.

[226] Cheng, D., Zhao, Z.-J., Zhang, G., Yang, P., Li, L., Gao, H., Liu, S., Chang, X., Chen, S., Wang, T. (2021). The nature of active sites for carbon dioxide electroreduction over oxide-derived copper catalysts. Nat Commun, 12, 1-8.

[227] Li, X., Yang, X., Zhang, J., Huang, Y., Liu, B. (2019). In Situ/Operando Techniques for Characterization of Single-Atom Catalysts. ACS Catal, 9, 2521-2531.

[228] Zhu, Y., Wang, J., Chu, H., Chu, Y.-C., Chen, H. M. (2020). In Situ/Operando Studies for Designing Next-Generation Electrocatalysts. ACS Energy Letters, 5, 1281-1291.

[229] Zhu, K., Zhu, X., Yang, W. (2019). Application of In Situ Techniques for the Characterization of NiFe-Based Oxygen Evolution Reaction (OER) Electrocatalysts. Angew Chem Int Ed, 58, 1252-1265.

[230] Qi, W., Yan, P., Su, D. S. (2018). Oxidative Dehydrogenation on Nanocarbon: Insights into the Reaction Mechanism and Kinetics via in Situ Experimental Methods. Acc Chem Res, 51, 640-648.

[231] Chang, C.-J., Hung, S.-F., Hsu, C.-S., Chen, H.-C., Lin, S.-C., Liao, Y.-F., Chen, H. M. (2019). Quantitatively unraveling the redox shuttle of spontaneous oxidation/electroreduction of CuO x on silver nanowires using in situ X-ray absorption spectroscopy. ACS Cent Sci, 5, 1998-2009.

[232] Petkov, N. (2013). In Situ Real-Time TEM Reveals Growth, Transformation and Function in One-Dimensional Nanoscale Materials: From a Nanotechnology Perspective. ISRN Nanotechnology, 2013, 893060.

[233] Vesborg, P. C., Chorkendorff, I., Knudsen, I., Balmes, O., Nerlov, J., Molenbroek, A. M., Clausen, B. S., Helveg, S. (2009). Transient behavior of Cu/ZnO-based methanol synthesis catalysts. J Catal, 262, 65-72.

[234] Li, Y., Zakharov, D., Zhao, S., Tappero, R., Jung, U., Elsen, A., Baumann, P., Nuzzo, R. G., Stach, E., Frenkel, A. (2015). Complex structural dynamics of nanocatalysts revealed in Operando conditions by correlated imaging and spectroscopy probes. Nat Commun, 6, 7583.

[235] Wang, G., He, C.-T., Huang, R., Mao, J., Wang, D., Li, Y. (2020). Photoinduction of Cu Single Atoms Decorated on $UiO\text{-}66\text{-}NH_2$ for Enhanced Photocatalytic Reduction of CO_2 to Liquid Fuels. J Am Chem Soc.